

Asymmetry of the Modern Human Endocranum

Lindsey M. Kitchell

Dissertation submitted in partial fulfillment of
the requirements for the degree of
MSc in Palaeoanthropology and Palaeolithic Archaeology
of University College London in 2015

UCL INSTITUTE OF ARCHAEOLOGY

Abstract

Hominin brain evolution is a topic of great interest in paleoanthropology. Details of this evolutionary process are typically inferred from endocasts. However, very little research has been done to *quantifiably* establish the relationship between an endocast and its corresponding brain. This study investigates this relationship using asymmetry of the entire endocranial surface. As the modern human brain is structurally asymmetric, the results of this study allow for a direct quantitative comparison of this characteristic between the two surfaces. In addition, because important aspects of behavior, such as handedness and language processing, are organized asymmetrically in the brain, it is of great interest to be able to see these same asymmetries on the endocranial surface.

Using innovative geometric morphometric techniques, this study quantified the degree and direction of asymmetry of the entire endocranial surface in adult modern humans. Results indicate the well-known petalia pattern of asymmetry extends beyond the frontal lobe to include the right temporal and anterior parietal regions. In addition to an anterior-posterior and lateral asymmetry, the petalias also differ in superior-inferior distribution. A rightward asymmetry of Broca's area was found, contradicting previous qualitative reports. A leftward asymmetry of the anterior cerebellum was also found and a rightward asymmetry of the temporal pole, as well as several other subtle asymmetries across the rest of the endocranial surface. The findings are compared with brain asymmetry research and the implications for brain evolution research are discussed.

Table of Contents

ABSTRACT	2
TABLE OF CONTENTS	3
LIST OF FIGURES	5
LIST OF TABLES	6
ACKNOWLEDGEMENTS	7
CHAPTER 1	8
1 INTRODUCTION	8
CHAPTER 2	11
2 LITERATURE REVIEW	11
2.1 THE STUDY OF HOMININ BRAIN EVOLUTION AND PALEONEUROLOGY	11
2.2 ENDOCASTS AND ENDOCRANIA	14
2.3 THE BRAIN-ENDOCAST RELATIONSHIP	22
2.4 STRUCTURAL BRAIN ASYMMETRY	24
2.5 ENDOCRANIAL ASYMMETRY	29
CHAPTER 3	34
3 OBJECTIVES AND HYPOTHESES	34
3.1 WHERE IS THE MODERN HUMAN ENDOCRANUM ASYMMETRIC AND WHAT IS THE VARIANCE AT THOSE LOCATIONS?	34
3.2 IS THERE SEXUAL DIMORPHISM IN THE MODERN HUMAN ENDOCRANIAL ASYMMETRY PATTERN?	34
CHAPTER 4	35
4 MATERIALS AND METHODS	35
4.1 SAMPLE	35
4.2 GEOMETRIC MORPHOMETRICS	35
4.3 DATA ACQUISITION AND PROCESSING	38
4.4 DATA ANALYSIS	46
CHAPTER 5	48
5 RESULTS	48
5.1 LANDMARK PRECISION	48
5.2 WHERE IS THE MODERN HUMAN ENDOCRANUM ASYMMETRIC AND WHAT IS THE VARIANCE AT THOSE LOCATIONS?	48
5.3 IS THERE SEXUAL DIMORPHISM IN THE MODERN HUMAN ENDOCRANIAL ASYMMETRY PATTERN?	61

CHAPTER 6	64
6 DISCUSSION	64
6.1 WHERE IS THE MODERN HUMAN ENDOCRANUM ASYMMETRIC AND WHAT IS THE VARIANCE AT THOSE LOCATIONS?	64
6.2 IS THERE SEXUAL DIMORPHISM IN THE MODERN HUMAN ENDOCRANIAL ASYMMETRY PATTERN?	68
6.3 LIMITATIONS	69
6.4 DOES THE ENDOCRANIAL ASYMMETRY OF MODERN HUMANS ACCURATELY CORRESPOND TO THE BRAIN ASYMMETRY OF MODERN HUMANS?	70
6.5 SUGGESTIONS FOR FURTHER RESEARCH	70
CHAPTER 7	72
7 CONCLUSION	72
REFERENCES	74

List of Figures

Figure 2.1 Cranial Capacities of Hominin Species	18
Figure 2.2 Shape differences between similarly sized endocasts of <i>Paranthropus</i> and <i>Australopithecus africanus</i>	19
Figure 2.3 Language areas of the brain	25
Figure 2.4 Petalia and Yakovlevian Torque	29
Figure 4.1 Semi-automated method for endocranial segmentation	39
Figure 4.2 Placement of the Fixed Landmarks	41
Figure 4.3 Placement of the Curve Outlines	43
Figure 4.4 Mirrored Endocasts	44
Figure 4.5 Surface Semilandmarks	45
Figure 5.1 Overall Amount of Endocranial Asymmetry	49
Figure 5.2 The Least and Most Asymmetric Specimens	50
Figure 5.3 Superior and Inferior Views of the Pattern of Endocranial Asymmetry (Surface Semilandmarks Only)	54
Figure 5.4 Left and Right Side Views of the Pattern of Endocranial Asymmetry (Surface Semilandmarks Only)	55
Figure 5.5 Anterior and Posterior Views of the Pattern of Endocranial Asymmetry (Surface Semilandmarks Only)	56
Figure 5.6 Superior and Inferior Views of the Pattern of Endocranial Asymmetry (All Landmarks)	57
Figure 5.7 Left and Right Side Views of the Pattern of Endocranial Asymmetry (All Landmarks)	58
Figure 5.8 Anterior and Posterior Views of the Pattern of Endocranial Asymmetry (All Landmarks)	59
Figure 5.9 Standard Deviation of the Mean Degree of Asymmetry of Each Landmark	60
Figure 5.10 Plot of the Mean Degree of Asymmetry and Standard Deviation at Each Landmark	61
Figure 5.11 Plot of the Female and Male Overall Asymmetry Values and Means ..	62
Figure 5.12 Landmarks with a Significant Difference in Degree of Asymmetry between Females and Males	63

List of Tables

Table 4.1 Description of the Fixed Landmarks	42
Table 4.2 Description of the Curves	43
Table 5.1 Overall Asymmetry Values	49

Acknowledgements

In full gratitude I would like to acknowledge the following individuals who advised, encouraged, and supported me in the pursuit of this dissertation:

At University College London, I would like to thank my supervisor Dr. Christophe Soligo for supporting and advising me in the development of this research and Dr. Andrew Garrard for encouraging me to pursue this degree. My thanks also goes to my fellow students for the inspiring discussions and conversations throughout this past year.

I would also like to thank the Open Research Scan Archive at the University of Pennsylvania Museum of Archaeology and Anthropology, Janet Monge, and P. Thomas Schoenemann for providing access to their CT scan data, without which this research would not have been possible. I am also thankful to Emma Sherratt, co-author of *Geomorph*, an R package for geometric morphometrics, for being willing to quickly adjust the code of *Geomorph* to my methodologies.

I am also very thankful to P. Thomas Schoenemann for introducing me to the field of paleoneurology and brain asymmetry.

I am also grateful to Alex Elvis Badillo for his support, encouragement, and willingness to listen, read, and talk through every single step of this dissertation.

Chapter 1

1 Introduction

The human brain is a highly complex and specialized organ, of which we have many unanswered questions. Perhaps one of the most intriguing mysteries surrounding the human brain is the process of its evolution. Determining when, how, and what factors influenced the developmental trajectory of the human brain is an important topic of inquiry in the field of paleoanthropology. Although a rough outline of the timing of major changes has been established, the answer to many fundamental questions are still unknown (Schoenemann, 2006). Researchers have inferred details of its evolution through indirect evidence gathered from the fossil record or comparative studies of extant primate brains (Holloway et al., 2004a, Holloway et al., 2009). Unfortunately, the brain is formed by soft tissue, which does not fossilize, leaving us with no direct evidence of the process of hominin brain evolution. Evidence from the fossil record (e.g. cranial capacity, gyri and sulci impressions) only provides information about the endocranial (inner) surface of the skull, not the brain directly (Holloway et al., 2004a, Holloway et al., 2009). To accurately interpret this information, we need to fully understand the relationship between the endocranial surface of the skull and the brain. We need to determine how well both surfaces reflect the shape of each other, how the relationship changes throughout development, and how the relationship transformed over time and between species.

Although the study of endocranial, or endocasts (casts of the endocranial surface), has been around since at least the early 1900's (Edinger, 1929, Holloway et al., 2004a), very little research has been done to quantifiably establish the relationship between an endocast and its corresponding brain (Fournier et al., 2011a). Consequently, the questions investigated in this dissertation were developed to begin quantifying this relationship. In particular, this study will determine where the modern human endocranum is asymmetric, as well as the variance of those asymmetries. It will also investigate sexual dimorphism in terms

of endocranial asymmetry, determining its presence or absence while measuring the degree of difference and mapping notable patterns. As the modern human brain has been shown to be structurally asymmetric (e.g. Good et al., 2001, Kitchell et al., 2013, Luders et al., 2004, Watkins et al., 2001), the results of this study will allow for a direct comparison of this characteristic between the two surfaces (brain surface and endocranial surface). Because important aspects of behavior, such as language processing, are organized asymmetrically in the brain, both functionally and structurally, it is of great interest to be able to see those same asymmetries on the endocranial surface (Dorsaint-Pierre et al., 2006, Falzi et al., 1982, Foundas et al., 1998, Schoenemann, 2006). If particular cortical, or structural, asymmetries of the brain are found to predict certain behaviors, the presence of the same asymmetry on the endocranial surface could allow us to infer those behaviors from fossil specimens.

While asymmetry of the endocranial surface has been studied previously, most of the methodologies used were only crudely quantitative, determined visually or by feel (Holloway and de la Coste-Lareymondie, 1982, LeMay and Kido, 1978), or consisted of linear measurements between a small number of points (Balzeau et al., 2012a, Balzeau et al., 2014). Others have used a surface-based method to quantify endocranial asymmetries, however they used MRI scans instead of CT scans to create the endocranial surface, a methodology of which is much less accurate than the methods carried out in the present study (Fournier et al., 2011a, Pechaud et al., 2006). Additionally, research has mostly focused on a specific pattern of macroscopic asymmetry referred to as petalias (the distinct protrusions of the right-frontal and left-occipital lobes (Toga and Thompson, 2003)) (Balzeau et al., 2012a, Fournier et al., 2011a), or on areas of the brain related to language, Broca's and Wernicke's areas (Balzeau et al., 2014, Holloway et al., 2004a), ignoring the rest of the endocranial surface.

In contrast, the innovative methodology used in this study will quantify asymmetry of the entire endocast. Using geometric morphometrics and in particular, a relatively new measurement protocol referred to as sliding semilandmarks (Gunz et al., 2005, Gunz and Mitteroecker, 2013), this study will determine shape differences between the entire right and left hemispheres of the

modern human endocranum. By placing semilandmarks across the entire surface of the endocast, I am able to quantify endocranial asymmetry in areas that are typically ignored in addition to those that have already been investigated.

The topic and questions explored in this dissertation are of particular interest to me because of my previous research on structural asymmetries of the modern human brain. As an undergraduate, I conducted a study using MRI scans and voxel-based morphometry to quantify the location and degree of structural asymmetries between the right and left hemispheres of the human brain (Kitchell et al., 2013). I also developed a small study examining the association between handedness and structural asymmetries of the human brain (Kitchell and Schoenemann, 2014). I wanted to quantify the asymmetry of the modern human endocranum in order to compare with the results of my brain asymmetry research, as well as to investigate the viability of predicting behavior from the endocranial surface. Furthermore, when I began learning about hominin brain evolution, one of the first questions I had was how accurately does the endocranial surface match the brain surface. I was shocked to find so little information in answer to this question. The results of this dissertation will contribute to closing this gap in paleoanthropological knowledge.

In Chapter Two of this document, “Literature Review”, I review the relevant literature surrounding the topic and present a concise background of information. In Chapter Three, “Objectives and Hypotheses”, I present a description of the main objectives and hypotheses that will be specifically addressed throughout the dissertation. In Chapter Four “Materials and Methods”, I describe the exact methodology followed for this study and the procedures used in data analysis. In Chapter Five “Results”, I present and describe the results obtained. In Chapter Six “Discussion”, the results are discussed and considered in context with the previous research reviewed in Chapter Two. In Chapter Seven “Conclusion”, I describe the conclusions that can be made on the results of this research. Lastly, a list of the literature that has been referred to in the dissertation is presented.

Chapter 2

2 Literature Review

In this chapter I review the published literature that is most relevant to the topic of this dissertation research. I start with an overview of the study of hominin brain evolution and the field of paleoneurology. I then discuss endocasts in more detail, including how they have been studied in the past and how that has changed with the new and improved technology in the recent decades. The next section reviews what is currently known about the relationship between the endocranial surface of the skull and the surface of the brain in modern humans. The fourth section discusses asymmetry in the structure and function of the modern human brain, how this is related to behavior, and how these asymmetries might be relevant to paleoanthropology. The final section reviews previous and current research specifically on asymmetry of the human endocranum.

2.1 The Study of Hominin Brain Evolution and Paleoneurology

One of the foremost defining characteristics of human evolution is the development of a larger, more complex brain. The encephalized human brain is the main organ responsible for many of the major behavioral differences between humans and our closest primate relatives. These differences include “the ability to learn and generate symbols, to manipulate symbol systems, to communicate with these systems (i.e. true language), to develop very high levels of intelligence, and to develop a large variety of skills, including artistic expression” (Holloway et al., 2004a, pg 3). Evidence from fossil hominin crania indicates that the hominin brain has tripled in size over the past 3-5 million years (Holloway et al., 2009, Schoenemann and Begun, 2013). Modern human not only have the largest brains in absolute size out of all of the living primates, but we also have unusually large brains for our body size (Falk, 2012, Schoenemann, 2006). Additionally, when the brains of modern humans are compared to the allometric relationship between the brain and body size of primates, the brains of modern humans are three times larger than expected for our body size (Schoenemann, 1997).

The remarkably large relative brain size clearly indicates that the size increase of the hominin brain is not simply due to a change in body size. Combined with the fact that large brains are slow to grow and very metabolically expensive, having such an enlarged brain suggests that brain expansion must have come with substantial benefits to counterbalance its cost. The expanded brains of our hominin ancestors likely played an important role in the evolution and success of the hominin lineage. Additionally, there is a positive correlation between brain size and level of cognitive ability in non-human primates that supports the idea that hominin intelligence increased with brain size (Deaner et al., 2007). In addition to size, the overall shape and organization of brain structures also changed over time. In hominins, changes of the overall brain shape and structure likely provided an opportunity for the manifestation of new cognitive abilities.

In order to understand the evolution of the human brain, it is necessary to identify not only what physical changes have occurred, but also why they have occurred. As the brain does not fossilize, we are limited to using indirect methods of analysis. One approach, the study of comparative neuroscience, examines and compares the brain structures of modern humans and other living primate species (Sherwood et al., 2009). Although there are prominent morphological and behavioral differences between humans and our primate relatives, according to phylogenetic research we are very closely related (The Chimpanzee Sequencing and Analysis Consortium, 2005). Comparisons between human and other primate, especially chimpanzee, brains may reveal the human brain specializations responsible for our unique cognitive abilities and behaviors (Falk, 2012, Sherwood et al., 2009). While comparative neuroscience can tell us what is currently different and unique about the modern human brain, it cannot tell us the process or timing of the development of those specific characteristics. Additionally, as modern humans are vastly different from the hominins who were alive immediately after the human-chimpanzee split, currently living non-human primates are the result of their own long evolutionary history and also likely very different from their own evolutionary ancestors (Falk, 2012, Venn et al., 2014).

Another approach and the one used in this dissertation research, is paleoneurology. The field of paleoneurology studies brain evolution through the analysis of endocasts. Although paleoneurology is relatively poor in data compared to comparative neuroscience, endocasts are able to provide us with information extant brains cannot, such as evolutionary changes within the hominin lineage and an estimate of the timing of those changes (Holloway et al., 2009). The study of endocasts has had a long and sometimes controversial history. Early publications mention observations of petrified mud in a pterodactyl skull by Oken in 1819, as well as in a crocodile skull by Owen in 1841 (Edinger, 1948b, Holloway et al., 2004a), but the field was formally established by Tilly Edinger in the early 1900's. Edinger advocated paleoneurology as a necessary correction to comparative neurology's tendency to use living brains as evidence of evolutionary lines of decent (Holloway et al., 2004a). Edinger's (1948a) monograph on the evolution of the horse brain has become a valuable and classic manuscript, while her 1929 and 1948 publications on the history of paleoneurology are important foundational texts, providing a needed critique of comparative neurology's misguided ideas on hominin brain evolution at the time (Edinger, 1929, Edinger, 1948b, Holloway et al., 2004a). The field grew quickly and in 1975 a posthumous annotated bibliography of Edinger's detailed records of the literature was published, containing nearly six times the number of publications as recorded by her earlier bibliographies published in 1929 and 1937 combined (Edinger, 1937, Edinger, 1974). Other valuable texts on the history of paleoneurology include Veronica Kochetkova's (1978) historical treatise and Joseph Connolly's (1950) book. More recent pioneers of human paleoneurology include Ralph Holloway, especially his comprehensive (2004a) volume on hominin endocasts, and Dean Falk, most well-known for her work on the *Homo floresiensis* endocast (Falk et al., 2005). Both are famous for their decades long debate over the identification and position of the lunate sulcus on the *Australopithecus africanus* specimen Stw 505's endocast (Falk, 2009, Falk, 2012, Holloway, 1985, Holloway et al., 2003, Holloway, 2015).

With the advent of new and better technology, the field of paleoneurology continues to expand and grow. Where researchers were previously taking hours

to hand make and reconstruct endocasts using silicon rubber and plaster, now an endocast can be created digitally within minutes using sophisticated visualization software. Advancement in statistical packages and morphometric techniques allow for the testing of more empirical and quantitative hypotheses, complementing earlier qualitative and visual methods (Holloway, 2015).

2.2 Endocasts and Endocrania

2.2.1 What is an Endocast or Endocranum?

An endocast is a physical (or virtual) cast of the endocranum of a skull (Holloway et al., 2004a). The endocranum is the interior of the neurocranium, or brain case area, of the skull. The terms endocast and endocranum will be used interchangeably throughout this dissertation as they refer to the same anatomical entity in different forms. It is important to remember that an endocast is not a cast of the brain surface nor does it give us any information about the internal structures of the brain. There are three layers of tissue, or meninges, that lie between the brain surface and skull (Holloway et al., 2004a). The first layer of tissue is the pia mater, a delicate membrane that firmly envelops the brain. The second layer is the arachnoid tissue, a fibrous membrane that contains the cerebrospinal fluid around the brain. The third layer of tissue is the dura mater, a dense, thick membrane with an outer layer that attaches to the bone of the neurocranium. These three layers of tissue prevent the brain from making an exact impression of its surface on the endocranum of the skull (Bruner et al., 2014, Holloway et al., 2004a).

An endocast can be natural, artificial (human-made), or virtual (computer generated) (Holloway et al., 2009, Holloway, 2009). A natural endocast occurs when the cranium is filled, through the foramen magnum or other foramina of the skull, with fine sediments after death. Eventually, these sediments are compacted and infiltrated by calcareous solutions and harden into a rock-like cast of the internal surface of the cranium (Holloway et al., 2004a, Holloway et al., 2009, Holloway, 2009). This process likely takes hundreds or thousands of years and the quality is dependent on the state of the cranium and any geological or taphonomic

changes that occur. The Taung, Sts 60, and SK 1585 endocasts are well known naturally made endocasts (Holloway et al., 2004a).

Artificial, or human-made, endocasts are physical casts made by applying a molding material such as liquid latex rubber or silicon rubber to the internal surface of the crania (Holloway et al., 2004a, Schoenemann et al., 2007). After the molding material dries, the material is pulled away from the cranial surface and extracted through the foramen magnum (if the cranium is complete). The rubber shell is then filled with plaster to stabilize its shape (Schoenemann et al., 2007). Often, especially in the case of fossil crania, the human-made endocast is partially incomplete. Incomplete casts are reconstructed by adding plasticene or modeling clay to the incomplete fragments and molding them to estimate the shape and overall size of the original, complete endocranum (Holloway et al., 2004a).

Recent technological advances have allowed for the creation of virtual endocasts using CT (computed tomography) scans (Balzeau et al., 2014, Bruner, 2007, Neubauer et al., 2009, Schoenemann et al., 2007, Tobias, 2001). This is especially useful for matrix-filled, distorted, or fragmented fossil specimens (Tobias, 2001, Zollikofer and León, 2013). A CT scan is essentially a set of density measurements of every point, or voxel, of a given three dimensional object or space (Schoenemann et al., 2007). The endocranial surface of a cranium can be delimited by thresholding the CT scan to only select voxels within the range of densities that corresponds to bone. A virtual endocast can then be selected by filling in the remaining volume of the braincase (Neubauer et al., 2009, Schoenemann et al., 2007). Once the endocranum is selected it can be rendered as a 3D model on a computer screen, or even 3D printed. The ability to create virtual endocasts has opened up the possibility for higher quality measurements, easier sharing, and allows us to test more quantitative hypotheses.

2.2.2 What Data Can We Acquire From Endocasts?

2.2.2.1 Size

Although endocasts are not an exact replica of the brain surface, they can still provide us with valuable data, such as general size, morphology, and some cortical details. Most notably, endocasts can provide an estimate of brain size

through determination of the cranial capacity. The cranial capacity is the volume of the endocranum. Using a specific algorithm, the cranial capacity can also be used to estimate brain weight (Holloway et al., 2004a). Cranial capacity and brain weight are sometimes used interchangeably although they are not identical, with the cranial capacity usually 10% larger (due to the inclusion of the meninges, cerebrospinal fluid, and cranial nerves) (Holloway et al., 2004a, Holloway, 2009). In the past, the cranial capacity of an endocast was measured by water displacement. The natural or human-made endocast was placed in a container of water and the volume or weight of the water that was displaced was measured (Holloway, 1981, Holloway et al., 2004a). Now, with the use of virtual endocasts, the volume of the 3D endocast model that is created can be measured instantly using various computer programs.

Estimates of brain size or cranial capacity combined with estimates of body size can be used to determine relative brain size (absolute brain size divided by body size) and encephalization quotients (actual brain size divided by the estimate of the average brain size for a mammal of the same body size) (Falk, 2012, Holloway et al., 2004a, Jerison, 1973, Zollikofer and León, 2013). Earlier researchers suggested that for all primates both the absolute brain size and its relative size compared to estimates of body size increased independently during evolution (Falk, 2012, Jerison, 1973, Radinsky, 1979). However, a more recent analysis has shown that while selective pressures for larger brains did begin early in primate evolution, they discovered that brain size also decreased independently in some lineages of old world monkeys, new world monkeys, and strepsirrhines (Montgomery et al., 2010). Additionally, while larger primates tend to have bigger *absolute* brain sizes, the accompanying larger body size tends to lead to a smaller *relative* brain size than the smaller-bodied primates (Falk, 2012). Partially due to the complicated relationship with body size, techniques such as the encephalization quotient have been developed to control for allometric scaling when studying brain size (Jerison, 1973, Schoenemann and Begun, 2013).

The cranial capacity is a fairly simple measurement, yet its implications are quite important. By comparing the cranial capacities of different hominin species and their close primate relatives, we can begin to develop a timeline of

evolutionary changes in hominin brain evolution (Figure 2.1). We know that the earliest hominin species, *Ardipithecus ramidus* (cranial capacity of around 300 cc (Suwa et al., 2009), *Australopithecus afarensis* (387 - 550 cc), and *Australopithecus africanus* (400 -560 cc) (Holloway et al., 2004a), had brains approximately the same size as living apes (*Pan troglodytes*, 280 - 450 cc; *Pan paniscus*, 275 - 380 cc; *Gorilla gorilla*, 350 -750 cc (Tuttle, 1986)), but with body sizes estimated to be smaller than modern chimpanzees (McHenry, 1992, Schoenemann and Begun, 2013). This indicates that despite a similar brain size, early hominins had an encephalization quotient larger than modern chimpanzees. The behavioral significance of encephalization quotients compared to absolute brain size is not very clear, however (Schoenemann and Begun, 2013).

Moving along the evolutionary timeline, the robust Australopithecines appear to experience a moderate increase in brain size. *Paranthropus aethiopicus* had a cranial capacity around 410 cc increasing to 475 - 545 cc in *Paranthropus boisei*, and 450 – 530 cc in *Paranthropus robustus* (Elton et al., 2001, Holloway et al., 2004a). In contrast, the *Homo* lineage experiences a dramatic increase in cranial capacity. Starting with *Homo habilis* with a cranial capacity between 509 - 687 cc, it continued to increase steadily with each new *Homo* species. For example, *Homo rudolfensis* had a cranial capacity from 752 – 825 cc, *Homo ergaster* from 750 – 848 cc, *Homo neanderthalensis* from 1172 to 1740 cc and early anatomically modern *Homo sapiens* from 1090 to 1775 cc (Holloway et al., 2004a, Schoenemann and Begun, 2013).

Given that a parallel increase in brain size is not seen in monkeys or other apes during the same time period, it is likely that there was something unique about the ecological niche of hominins that either selected for larger and larger brains or provided an increase in the acquisition of resources necessary to handle the higher metabolic costs of a bigger brain (Schoenemann and Begun, 2013).

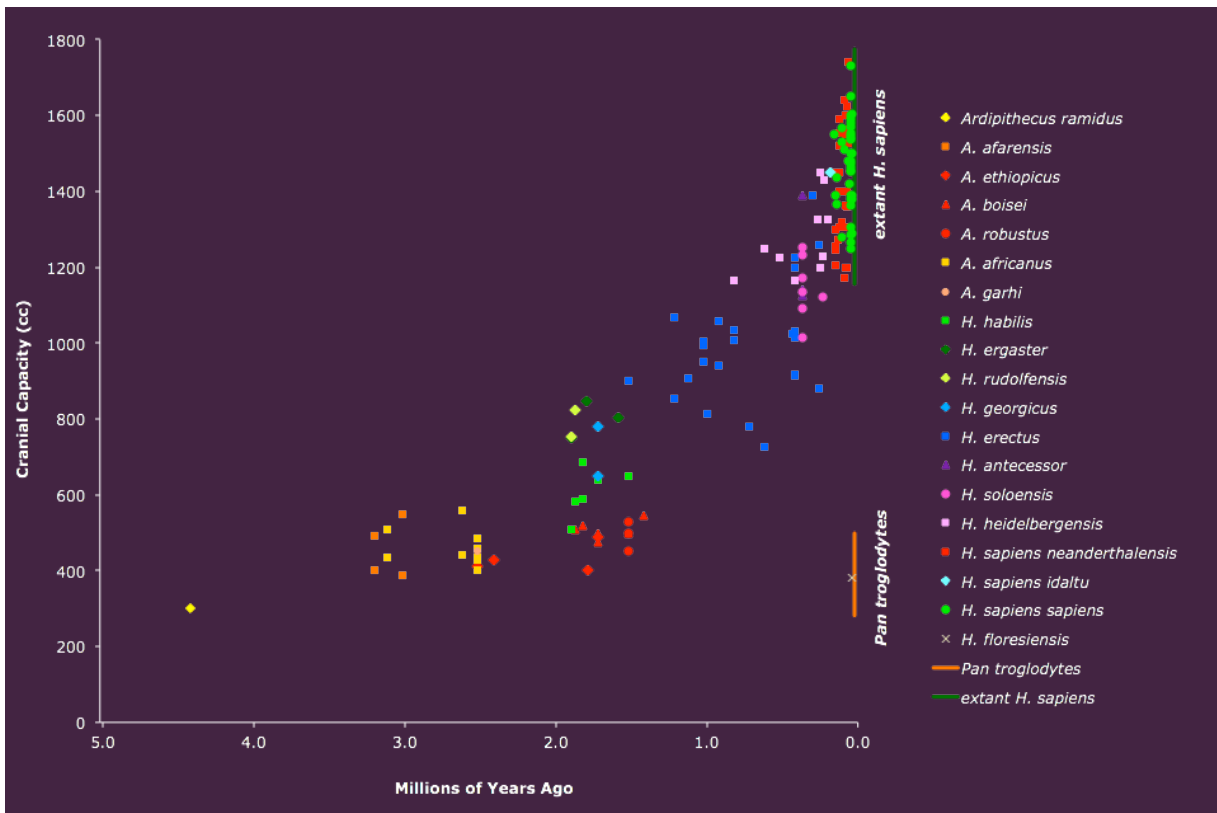


Figure 2.1 Cranial Capacities of Hominin Species. Figure created by P. Thomas Schoenemann (personal communication) and data collected from Holloway et al. (2004a) and Schoenemann (1997).

2.2.2.2 Morphology

In addition to overall size, endocasts can also provide us with information about the overall shape of the brain and relative size and shape of the lobes of the brain. For example, despite a similar brain size, endocasts of *Paranthropus* specimens were found to have relatively pointed frontal lobes and stubby temporal lobes in comparison with *Australopithecus* specimens (Figure 2.2) (Falk et al., 2000, Falk, 2009, Falk, 2012). Studies comparing *Homo erectus*, *Homo neanderthalensis*, and *Homo sapiens* endocasts found that the parietal regions have expanded more extensively than the other regions of the brain (Bruner, 2010, Bruner et al., 2003, Bruner, 2004).

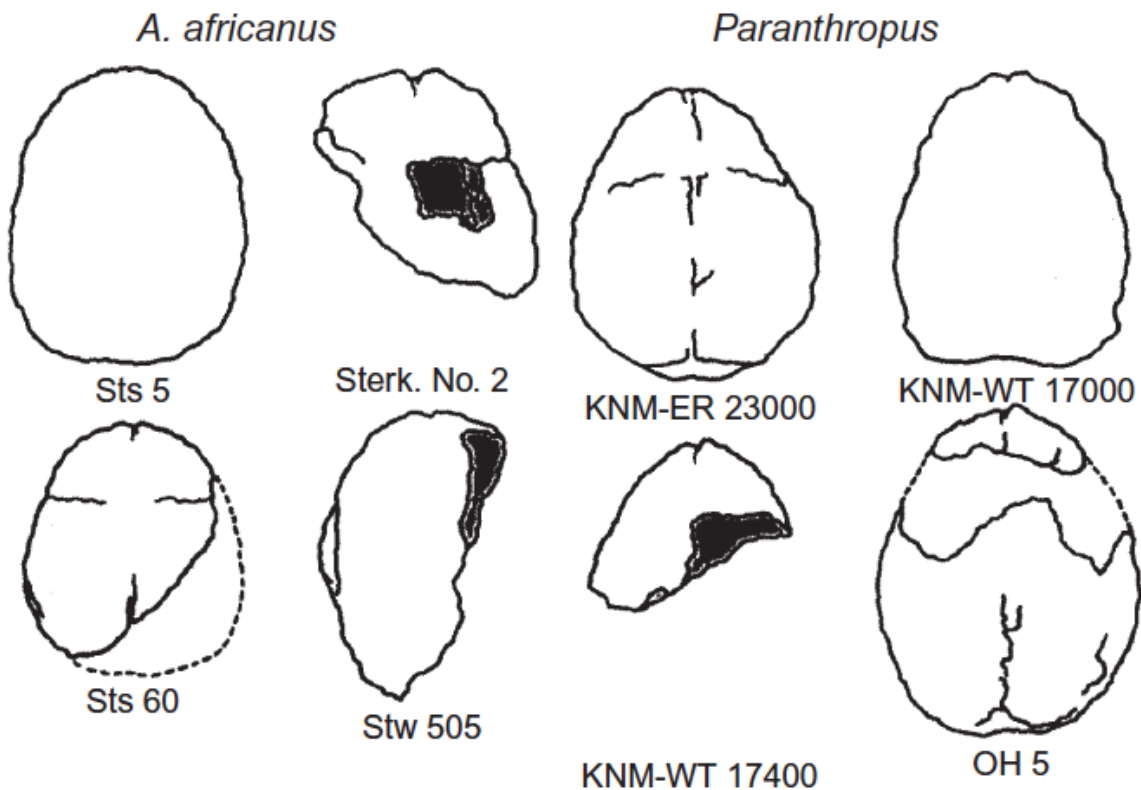


Figure 2.2 Shape differences between similarly sized endocasts of *Paranthropus* and *Australopithecus africanus*. Figure and caption reproduced from Falk (2012).

The methods used to quantify endocranial shape have changed drastically in the past few decades. Traditionally, endocasts were measured in chords and arcs between landmarks (Connolly, 1950, Grimaud-Hervé, 1997, Holloway et al., 2004a, Kochetkova, 1978). Common measurements were cerebral length, maximum breadth, cerebral height, and width of the cerebellum (Holloway et al., 2004a). It was also occasionally possible to measure distances between certain sulci impressions and compare those to measurements on brains. Along with these measurements, visual and qualitative observations on shape were made (Holloway, 1970, Holloway, 1981). Researchers made notes on the roundness of the prefrontal lobes and how far the cerebral hemispheres hung over the cerebellar lobes. The shape of the third inferior frontal convolution, an area that includes Broca's area, was analyzed as having either a more human-like or pongid-like form (Holloway et al., 2004a).

With the advent of virtual endocasts as well as advanced techniques like geometric morphometrics, morphological observations can be analyzed more quantitatively and can include the entire endocranial shape (Bienvenu et al., 2011, Neubauer, 2014). New questions can be asked that were not previously answerable. Innovations such as the development of semilandmark techniques (Gunz et al., 2005, Gunz and Mitteroecker, 2013), enable the inclusion of curves and surfaces in shape analyses. Recent publications have used landmark and semilandmark based morphometric techniques with virtual endocasts to compare the pattern of shape changes between the brain and endocranial surface throughout ontogeny (Neubauer et al., 2009, Neubauer et al., 2010, Ventrice, 2011). Additionally, landmark-based geometric morphometric techniques can estimate the location of missing areas in incomplete fossil specimens and correct distortions (Gunz et al., 2009, Neubauer, 2014).

2.2.2.3 Reorganization and Brain Convolutions

Convolutional details of the brain surface are also occasionally visible on the endocranial surface, in spite of the meningeal tissues between the two surfaces. Although it varies greatly between individuals and even hemispheres, certain gyri and sulci are sometimes imprinted on the endocranial surface (Falk, 2012, Holloway et al., 2004a, Holloway et al., 2009, Tobias, 1987). Classifying the imprints is difficult and often ambiguous, however. In the past, interpretation of the convolutional imprints was generally done by trying to visually match up illustrations of the modern human or chimpanzee brain with the subtle indentations on the endocast (Connolly, 1950, Holloway et al., 2004a). Recently, the use of virtual endocasts has made it easier to detect these subtle grooves (Carlson et al., 2011, Zollikofer and León, 2013).

Two particular regions of the endocranum have been studied in depth due to their important role in the reorganization of the hominin brain. These are the primary visual striate cortex and the third inferior frontal convolution. Throughout hominin evolution the size of the primary visual cortex decreased relative to the whole brain. In absolute size, the modern human primary visual cortex is approximately 1.5 times larger than a chimpanzee's; however, its volume is about

121% less than would be expected for a primate with the same brain weight (De Sousa et al., 2010, Holloway et al., 2003, Holloway et al., 2004a, Stephan et al., 1981). Furthermore, in all great apes the primary visual cortex is outlined anteriorly by the lunate sulcus. In modern humans this sulcus is typically not present, and when it is, it is in a much more posterior location (Allen et al., 2006, Connolly, 1950, Holloway, 1985, Holloway et al., 2003, Holloway et al., 2004a). While we know that a reduction occurred in the primary visual cortex, the timing of this change is very controversial.

Holloway (e.g., 1985, 2003, 2004a) believes that this reduction and other reorganizational changes occurred before an increase in brain size. He believes that the lunate sulcus was in a posterior, human-like position in the early Australopithecine brain, citing the estimated position of the sulcus on several endocasts (Schoenemann and Begun, 2013). In particular, Holloway has suggested a posterior lunate sulcus on *Australopithecus afarensis* specimen AL 162-28, and *Australopithecus africanus* specimen Stw 505 (Holloway, 1983a, Holloway, 1986, Holloway et al., 2004b). Falk (e.g., 1985, 2012) disagrees, arguing that the reduction in the primary visual cortex occurred later in evolutionary time, after the brain began to expand. She is also not convinced that the sulcus Holloway identifies is indeed the lunate sulcus and does not believe that there is any evidence the lunate sulcus was shifted posteriorly before disappearing. Falk (2012) suggests instead that an increase in brain size led to the loss of the lunate sulcus due to an increase in interconnections between the areas of the brain it separated. While they may disagree on the timing, Falk and Holloway do not dispute the fact that a reduction of the primary visual cortex did occur at some point in the hominin lineage.

The other region that has been studied extensively is the third inferior frontal convolution, also sometimes referred to as Broca's cap. This region is significant because it includes Broca's area of the brain. Broca's area plays an important role in language production for modern humans. Qualitative studies suggest that from early *Homo* species on, Broca's cap is larger on the left side of the endocast (Falk, 1983, Holloway, 1983b, Holloway, 1995, Tobias, 1987). Conversely, a more recent quantitative study of the third inferior frontal

convolution across all species of hominins actually found a reduction in size of the left side, while the right side projects more laterally and anterior-posteriorly (Balzeau et al., 2014). The reduction led to a more globular and defined Broca's cap on the left side, making it appear larger visually.

2.3 The Brain-Endocast Relationship

As mentioned earlier in this chapter, there are three layers of tissue, called the meninges, between the brain and the skull that prevent the brain from creating a perfect imprint on the endocranial surface. Although we know that an endocast is not a perfect representation of the brain, not much research has been done on *quantifying* just how different or similar the endocranial surface is from the brain surface in humans. In the past, endocasts and brains were compared visually. With recent improvements in technology, we have the opportunity to study this relationship in new ways.

Symington (1916) initiated the discussion on whether or not we could actually retrieve useful information from the endocranial surface. He compared the impressions on endocasts of modern humans to the fissures and convolutions of the corresponding brains. Symington concluded that "The simplicity or complexity of the cerebral convolutions cannot be determined with any degree of accuracy from endocranial casts even in complete skulls much less on reconstructions from imperfect skulls" (Symington, 1916, pg 130). His findings led him to doubt the interpretations and conclusions drawn from endocasts by other researchers of the same time period, such as Boule and Anthony (1911) and Smith (1913).

Le Gros Clark et al. (1936) studied the endocranial casts of six chimpanzees and compared them with the corresponding brains. Their results led them to essentially the same conclusion as Symington. In their paper they conclude, "the preceding account shows that very little information can be extracted in regard to sulcal pattern from the majority of our endocranial casts of the chimpanzee" (Le Gros Clark et al., 1936, pg 267). Connolly (1950) compared the endocranial casts of both anthropoid and human crania with the corresponding brains. He concluded that "the endocranial cast reproduces the form of the brain quite

closely”, however “in great measure the results of this study support the views of Symington” in terms of reproducing fissure and convolutional markings (Connolly, 1950, pgs 322-323). He also found that the degree of fissure and convolution impressions varied in relation to age or the developmental stage of the brain. Connolly (1950) suggested that differences between humans and anthropoids in the impressions on the endocranial surface are likely due to different rates of brain development and closing of cranial sutures. Falk (1980, pg 526) states that “latex endocasts prepared from selected prosimians and monkey skulls reproduce clear sulcal patterns; pongid and human skulls (even if carefully selected) do not.”

Lately, the hesitation to make conclusions about the brain using the endocranial surface has been set aside. Many recent publications use endocranial landmarks as representatives of brain structures with limited discussion of the brain-endocast relationship (e.g. Bruner, 2004, Bruner and Holloway, 2010, Neubauer et al., 2010). Bruner et al. (2015), however, investigated the spatial relationship between midsagittal cranial and cerebral landmarks and found that the spatial correlation between cerebral and cranial elements is very weak. The authors also state: “Although brain and braincase show a reciprocal relation in terms of size (volume) and shape (curvature), the position of their anatomical elements is sensitive to independent factors. This independence must be considered when evaluating brain reconstruction in fossil species” (Bruner et al., 2015, pg 8). Fournier et al. (2011a) also mapped the distance between the brain and endocranial surface and found the distance to be greatest at the front and top of the brain, but minimal at the sides.

Because endocasts are one of the only sources of evidence we can use to answer questions about hominin brain evolution, it is necessary that we fully characterize and understand the relationship between the brain and endocranial surface. Unfortunately, it is very difficult to obtain both brain (via MRI) and endocranial (via CT) data from the same individuals due to high costs, logistics, and risk of X-ray exposure (Bruner et al., 2015). Instead, aspects of the brain and endocranial surfaces are typically studied using different data sets and compared

using population or sample averages. One particular characteristic of these surfaces that is interesting and useful to compare is asymmetry.

2.4 Structural Brain Asymmetry

Although both hemispheres of the modern human brain are similar in weight and volume, the distribution of tissue differs substantially between them. This asymmetry in tissue distribution is thought to be the result of several developmental, evolutionary, and genetic factors. Many of the local asymmetries of the brain have also been attributed to certain behavioral traits such as handedness, auditory perception, motor preferences, and sensory acuity (Toga and Thompson, 2003). Brain asymmetries, if functionally relevant, may have important evolutionary implications - particularly if they are likely to produce indications on endocasts. Petalias (the asymmetric forward protrusion of the right frontal lobe and posterior protrusion of the left occipital lobe) are visible on an endocast (Holloway et al., 2004a) and because they may be correlated with handedness (Bear et al., 1986, LeMay, 1976), they are potentially useful for assessing handedness of fossil specimens. Hemispheric asymmetry in language areas is especially interesting for human evolution. If it can be demonstrated that the classical language areas are larger on the left hemisphere than the right - which would match functional asymmetries - it would potentially allow for more grounded studies of language evolution from fossil specimens.

2.4.1 Local Asymmetries:

The earliest observations of lateralized specialization were found in areas of the brain relevant to language. In the late 19th century, Paul Broca and Carl Wernicke described several patients with lesions in two different regions of the left hemisphere that had different language deficits (Broca, 1861, Wernicke, 1874). Broca's patients had damage to the inferior frontal gyrus and had difficulty producing fluent speech, while Wernicke's patients had damage to the posterior superior temporal gyrus and had difficulty producing comprehensible speech (Figure 2.3). Subsequent studies have shown that damage to Broca's area on the left results in at least temporary loss of fluent language function, while injury to

the same area in the right hemisphere rarely produces any speech problems at all (Mohr et al., 1978). It is therefore generally accepted that these areas in the left hemisphere play a role in language and speech processing in the brain.

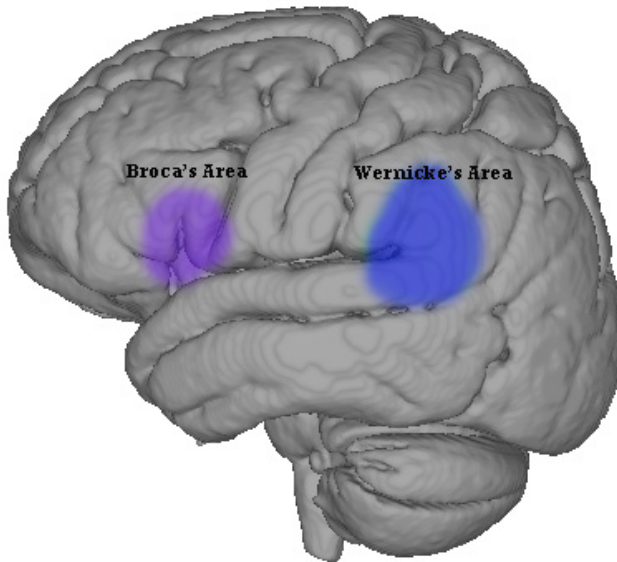


Figure 2.3 Language areas of the brain. Location of Broca's Area (purple) and Wernicke's Area (blue).

There are two regions within Broca's area that have consistently been demonstrated to be asymmetric: the pars triangularis and pars opercularis. Using volumetric MRI scans of 11 subjects, Foundas et al. (1996) found a significant leftward asymmetry in the pars triangularis in subjects who were right handed and it was known that their left hemisphere was specialized for language (this is referred to as language lateralization). The one left handed subject with language lateralized to the right, had a rightward asymmetry of the pars triangularis. In a later study, Foundas et al. (1998) repeated their methods on a larger sample size (32 individuals) and found a significant leftward asymmetry in the pars triangularis in both right and left handed subjects, but reduced in the left handed subjects. Foundas et al. (1998) also demonstrated a structural asymmetry in the pars opercularis. A significant leftward asymmetry was found to be more common in right-handed subjects, while a significant rightward asymmetry was found in

the left handed subjects. A clear correlation was found between asymmetry of the pars opercularis and handedness.

The planum temporale in the temporal lobe (part of Wernicke's area) is another region that has been consistently demonstrated to be asymmetric. Foundas et al. (1994) measured the length of the planum temporale on MRI scans of 12 patients whose language lateralization was known. The planum temporale was found to be longer in the left hemisphere of all right handed subjects with language lateralized to the left. The one non-right handed subject had language lateralized to the right and a rightward asymmetry of the planum temporale. In a similar study with a sample size of 67 subjects, the planum temporale was demonstrated to be significantly larger in the left hemisphere than the right for 72% of their subjects (Foundas et al., 2002). Watkins et al. (2001) also showed an overall significant leftward planum temporale asymmetry in their MRI study of 142 subjects. The asymmetry was more pronounced in the right-handed subjects. Another study measured the volume of the planum temporale in MRI scans of epilepsy patients and found leftward structural symmetries (Dorsaint-Pierre et al., 2006). However, these planum temporale asymmetries did not correlate with language lateralization as seen in Broca's area or as earlier research by Geschwind and Levitsky (1968) suggested. Recent studies have also revealed similar left-biased asymmetries in the planum temporale of apes (Gannon et al., 1998), further suggesting that this asymmetry is not connected to human language *per se*.

Early studies of neuroanatomical asymmetry were done post-mortem, and typically focused on particular regions of interest (ROIs), such as the inferior frontal gyrus, pars opercularis, pars triangularis, and the planum temporale (Albanese et al., 1989, Falzi et al., 1982, Geschwind and Levitsky, 1968, Harasty et al., 1997, Wada et al., 1975). More recent MRI-based studies, such as those discussed above, have also tended to focus on the same ROIs (Falk et al., 1991, Foundas et al., 2001, Foundas et al., 1998, Keller et al., 2007, Steinmetz and Galaburda, 1991). Watkins et al. (2001) argue that these regions of interest studies have methodological limitations involving how structural/anatomical boundaries were defined, leading to low intra- and inter-rater reliability. It is likely that some

biased was introduced due to having to manually delineate the ROIs. In response, several *in-vivo* whole brain asymmetry studies that used high resolution MRI have been published. These have typically used a variant of voxel-based morphometry to determine asymmetry (Good et al., 2001, Hervé et al., 2006, Luders et al., 2004, Watkins et al., 2001). These techniques quantify the degree to which individual voxels, or points, on one side of the brain would need to be adjusted in order to match corresponding voxels on the other side. They depend on accurate matching of corresponding voxels on both sides of the brain. To the extent that this matching can be semi-automated, the method can limit subjectivity and inter-observer error. They can also assess asymmetry on a global scale, allowing many areas (including grey and white matter) to be assessed at the same time and eliminating the need to manually define areas.

All four voxel based morphometric studies published to date replicate previous findings of frontal and occipital petalias, as well as asymmetries of the planum temporale, Heschl's gyrus (also part of Wernicke's area), cingulate gyrus, and caudate nucleus (Good et al., 2001, Hervé et al., 2006, Luders et al., 2004, Watkins et al., 2001). Each study found numerous additional areas that were asymmetric, but results were not always consistent between studies. Unlike the earlier volumetric MRI studies, none of the voxel based morphometric studies reported asymmetries in Broca's area specifically, but most did report a number of areas in the inferior frontal that were leftward asymmetric, including the anterior and lateral orbital gyri. My own research, Kitchell et al. (2013), used a novel voxel based morphometric approach with MRI scans to quantify the location and degree of left-right asymmetries in modern human brains. Our analysis confirmed the leftward occipital/rightward frontal petalias asymmetry, as well as a leftward asymmetry of the planum temporale and Heschl's gyrus. On the surface, we found a significant leftward asymmetry of the anterior cerebellum and rightward asymmetry of the posterior cerebellum, as well as two regions of leftward asymmetry within the motor cortex. Unlike the other voxel based morphometric studies, we did find a leftward asymmetry within Broca's area. We also found a very large continuous region of rightward asymmetry in the middle temporal gyrus, a region that is thought to be important in auditory perception,

such as voice processing (Kriegstein and Giraud, 2004, Samson and Zatorre, 1994).

2.4.2 Global Asymmetries

In addition to local asymmetries of specific brain areas, the modern human brain is asymmetric on a global scale. Although both hemispheres are similar in volume and weight, the right hemisphere protrudes more anteriorly than the left and the left hemisphere protrudes more posteriorly than the right. Additionally, the right frontal region is often wider than the left frontal and the left occipital region is wider than the right occipital (Toga and Thompson, 2003). As mentioned before, these protrusions are known as petalias and often produce imprints on the endocranial surface of the skull (Figure 2.4) (Holloway and de la Coste-Lareymondie, 1982, LeMay, 1976, LeMay and Kido, 1978). Another distortion of the brain hemispheres, the Yakovlevian anticlockwise torque, includes the petalias with the addition of the left occipital lobe extending across the midline. This distortion bends the interhemispheric fissure towards the right hemisphere (LeMay, 1976, Toga and Thompson, 2003).

The petalia asymmetry pattern has shown up in the results of many modern human brain asymmetry studies (e.g. Good et al., 2001, Hervé et al., 2006, Kitchell et al., 2013, Luders et al., 2004, Thompson et al., 2001, Toga and Thompson, 2003, Watkins et al., 2001). Furthermore, the direction of the petalia asymmetry pattern has been shown to correlate with handedness and to differ between males and females (Bear et al., 1986, Galaburda et al., 1978, LeMay, 1976, LeMay et al., 1982, LeMay and Kido, 1978). Bear et al. (1986) found that non-right handed subjects show a reduction or reversal of the petalia asymmetry. Male subjects showed greater degrees of petalia asymmetry than female subjects, and females were more likely to exhibit reduced or reversed petalia asymmetries. Additionally, global brain asymmetries may be correlated with other structural asymmetries. Barrick et al. (2005) found a significant correlation between a left planum temporale asymmetry and the torque of the right frontal and left occipital lobes. Pilcher et al. (2001) found a similar correlation between planum temporale asymmetries and right frontal, left occipital volumetric asymmetries in great apes.

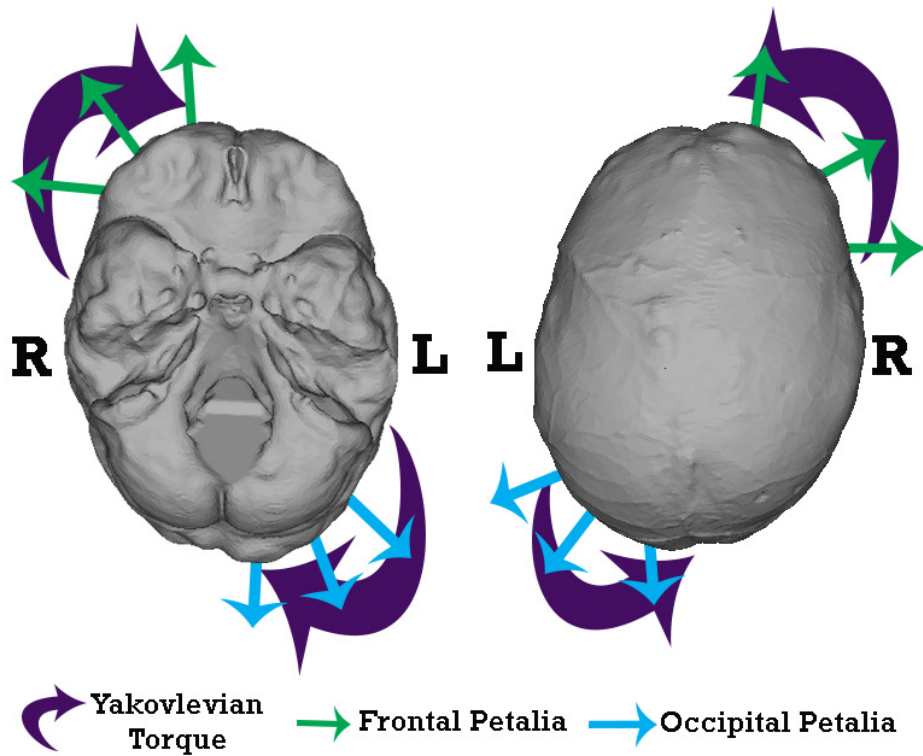


Figure 2.4 Petalias and Yakovlevian Torque. An example of the right frontal and left occipital petalias and Yakovlevian torque on the endocranial surface of one of the specimens used in this study.

2.5 Endocranial Asymmetry

The development and occurrence of anatomical asymmetries of the endocranial surface has been studied extensively in the hominin fossil record as an attempt to trace the evolution of cognitive capacities and behaviors (Balzeau et al., 2012b). Of particular interest has been the petalias pattern of right frontal and left occipital asymmetry, due to its correlation with handedness, as well as an asymmetry of Broca's cap, an area roughly corresponding to Broca's area of the brain. Early research on endocranial asymmetry, like research on other aspects of endocast size and shape, was mostly qualitative. Differences between the two hemispheres of the endocranum were determined visually or by feeling the physical surface of the endocast (e.g. Holloway, 1981, Holloway et al., 2004a). More recently, specific endocranial asymmetries have been reevaluated using qualitative methods (Balzeau et al., 2012a, Balzeau et al., 2014).

2.5.1 Petalias

As discussed above, the hemispheres of the modern human brain are asymmetric, the right frontal lobe protrudes more anteriorly and laterally than the left frontal lobe and the left occipital lobe protrudes more posteriorly and laterally than the right occipital lobe (Figure 2.4). Evidence of this petalial pattern on hominin endocasts was first noticed on the endocranial cast of the Neanderthal La Chapelle-aux-Saints skull (Boule and Anthony, 1911, LeMay, 1976). LeMay (1976) observes hemispheric asymmetries on seven specimens of *Homo erectus* and early *Homo sapiens*. Holloway (1981) mentions evidence of petalias when he describes the endocasts of Neanderthal cranial specimens Spy I, Spy II, Djebel Ithroud I, and of a *Homo erectus* specimen from Salé, Morocco. All four endocasts showed a right frontal/left occipital petalia, according to visual assessment. Holloway and de la Coste-Lareymondie (1982) conducted a very extensive qualitative study on petalial asymmetry in hominoids. The entire sample of endocasts was assessed simply for the presence or absence of petalias in the frontal and occipital regions. They found that the right frontal/left occipital particular petalial pattern was only consistently present in modern and fossil hominins (*Australopithecus*, *Homo erectus*, *Homo Neanderthalensis*). Non-human primates also occasionally showed a petalial pattern, but not always in the same direction or to the same degree of consistency as in hominins. Tobias (1987) found visual evidence of right frontal/left occipital petalias on the *Homo habilis* specimen OH 16, but a rightward occipital petalia on two other *Homo habilis* specimens OH 24 and OH 13.

Balzeau and Gilissen (2010) and Balzeau et al. (2012a) investigated the presence of petalial asymmetry on virtual endocasts of modern humans, fossil hominins, and great apes using a quantitative landmark-based method. They measured the anterior-posterior projection of the frontal and occipital lobes by placing a landmark at the most protruding point on the right and left side of both lobes. Asymmetry was measured in relation to a plane defined by the location of the glabella, inion, and basion on the skull. Their results indicate that great apes and anatomically modern humans display a similar petalial pattern but great apes have a lower amount of variation and a lower degree of asymmetry. The fossil

crania studied suggested an intermediate pattern between great apes and modern humans for degree of petalia asymmetry evidence (Balzeau et al., 2012a). It appears that it is the degree of petalial asymmetry more so than the direction of the petalias that differentiates modern humans, fossil hominins, and great apes. Fournier et al. (2011b) developed an automated surface-based technique to evaluate global brain asymmetries using endocasts created from MRI scans of modern humans and chimpanzees. Their results found the familiar right frontal/left occipital asymmetry pattern in both humans and chimpanzees, however in chimpanzees, the areas with the greatest difference between hemispheres were located laterally instead of at the tip of the lobes.

Balzeau et al. (2012b) examined surface area asymmetries of regional areas of the endocranial surface within the genus *Homo*. Their results found very little difference in regional surface asymmetries between the fossil species of *Homo* and anatomically modern *Homo sapiens*. The right hemisphere as a whole was found to have a larger surface area than the left hemisphere. Additionally, the right frontal lobe, the right parieto-temporal lobe, and the left occipital lobe all had a larger surface area than the same region of the opposite hemisphere (Balzeau et al., 2012b).

2.5.2 Broca's Cap

An asymmetry of Broca's area is of particular interest in hominin evolution because of the area's functional link to language capabilities. Broca's area asymmetries have been measured in the modern human brain, but applying these findings to endocasts is complex. The area examined on an endocast is actually slightly inferior to Broca's area of the brain and therefore is better referred to as Broca's cap. It is suggested that an elaboration of Broca's cap is visible on the left hemisphere of some fossil hominin endocasts (e.g. Falk, 1983, Holloway, 1983a, Holloway, 1995, Holloway et al., 2004a, Tobias, 1987). Broca's cap was first introduced by Anthony (1913) in his description of the third inferior frontal convolution of the La Quina endocast. Tobias (1975), Holloway (1983b), and Falk (1983) argue that Broca's cap is present beginning with early *Homo*. Broadfield et al. (2001) report asymmetrical Broca's caps on the endocast of *Homo erectus*.

specimen Sambungmacan 3. They found that the width of the cap is larger in the right hemisphere, but the length is longer in the left.

Most of these studies, however, have been purely descriptive and concerned with the lateral or inferior projection of Broca's cap. Until the Balzeau et al. (2014) study, no quantitative description of Broca's cap had been done. This is important because it is likely that visual descriptions have been influenced by global asymmetries and overall brain shape. Balzeau et al. (2014) developed methods to quantify different aspects of the third convolution on modern human, hominin, and great ape endocasts, independent of global asymmetries. They placed three anatomical landmarks on locations that were easily recognized on all specimens, including: the most anterior extension of the third frontal convolution, the maximal curvature of the triangular part that characterizes the lateral extension of the convolution, and the upper aspect of the Sylvian valley between the opercular part of the convolution and the temporal lobe. The position of these points was quantified and compared in several different ways. Their results indicate a global bilateral increase in the size of the third frontal convolution across all hominin species throughout hominin evolution. Balzeau et al. (2014) also indicate that the generally accepted leftward Broca's cap asymmetry is incorrect. Instead, it appears that the left side reduced in size compared to the right but became more clearly defined. As a whole, the third frontal convolution projects more laterally and antero-posteriorly in the right hemisphere, making the left convolution appear more globular and well defined. Balzeau et al. (2014) also found that the Broca's cap asymmetry pattern visible in *Pan paniscus* was very similar to the pattern seen in hominins, only differing in the degree of asymmetry.

2.5.3 Other Asymmetries

There is virtually no discussion of other possible regions of asymmetry on hominin endocasts. It is possible that no other endocranial asymmetries exist, but a more likely reason for this absence is a combination of a lack of interest and lack of sufficient methodologies to study other regions. Both petalial asymmetry and Broca's area have clear behavioral implications (e.g. handedness and language) and those behaviors are particularly interesting to paleoanthropologists. Whereas

other regions with less clear implications or less interesting functions were probably not considered worth researching. Additionally, until recently research on endocranial asymmetry was highly dependent on visual identification. Many of the areas of asymmetry on the modern human brain surface are small and a corresponding asymmetry on the endocranial surface would be extremely difficult to discern visually. Before the development of geometric morphometrics and surface semilandmarks it was not possible to quantitatively measure areas of endocasts that did not have clearly visible landmarks (Gunz et al., 2005, Gunz and Mitteroecker, 2013).

Chapter 3

3 Objectives and Hypotheses

The main objective of this dissertation is to use geometric morphometrics to determine relative shape differences between the left and right hemispheres of the modern human endocranum, in order to better characterize the relationship between the endocranial surface and brain surface of modern humans. This study will focus on endocranial asymmetries and their association with brain surface asymmetries. The following specific questions, with their respective hypotheses, will be addressed throughout this dissertation:

3.1 Where Is the Modern Human Endocranum Asymmetric and What is the Variance at Those Locations?

Hypothesis 1: The modern human endocranum will show a petalial pattern of asymmetry with the right frontal and left occipital lobes protruding out more than the opposite hemisphere.

Hypothesis 2: The area of Broca's cap will be larger on the right side of the endocranum, but more globular in appearance on the left side.

3.2 Is There Sexual Dimorphism in the Modern Human Endocranial Asymmetry Pattern?

Hypothesis 3: Male specimens will have a higher degree of global petalia asymmetry compared to the female specimens.

Chapter 4

4 Materials and Methods

4.1 Sample

The data used in this study consists of high resolution computed tomographic (CT) scans of crania from 28 adult modern human specimens, including 14 males and 14 females ranging from 25 to 30 years of age. The CT scans were obtained from the Open Research Scan Archive (Monge and Schoenemann, 2011). The Open Research Scan Archive is an online CT scan database that contains CT scans of human and non-human crania from the University of Pennsylvania Museum of Archaeology and Anthropology as well as several other institutions. The crania used in this study are from the Samuel George Morton Collection (Monge and Schoenemann, 2011). The age and sex of each specimen were taken from the descriptions listed in the archive. A subset of 100 crania (50 females and 50 males) was chosen randomly (within the age and sex criteria) from the collection for potential use. Several of the selected crania were not suitable for use due to deformation or taphonomic damage and were therefore excluded from this study, leaving a total of 28 crania for analysis.

4.2 Geometric Morphometrics

Relative shape differences between the left and right hemispheres of the modern human endocranum were determined using geometric morphometrics. Geometric morphometrics is a method of shape analysis based on the statistical analysis of landmark coordinates (Adams et al., 2004, Bookstein, 1997, Gunz and Mitteroecker, 2013, Mitteroecker and Gunz, 2009, Slice, 2007). A basic geometric morphometric analysis consists of three general steps: (1) Landmark coordinates are collected on each specimen; (2) The landmark coordinates for all specimens are superimposed, aligned, and scaled to the same size (referred to as a Procrustes superimposition); (3) Similarities and differences in shape are analyzed using various methods.

4.2.1 Fixed Landmarks and Semilandmarks

As defined in Zelditch et al. (2004), landmarks “are discrete anatomical loci that can be recognized as the same loci in all specimens in the study” and they are often placed on bony processes, sutures, or foramina. However, not all shapes can be accurately described using traditional, or fixed, landmarks. It is difficult to represent smooth curves and surfaces using fixed landmarks because they lack distinct structures and the position of the landmark along the curve or surface may not be homologous across specimens (Gunz and Mitteroecker, 2013).

Instead, sliding semilandmarks can be used. The method of sliding semilandmarks uses sets of points to represent curves and surfaces and establish a geometric homology between specimens (Gunz et al., 2005, Gunz and Mitteroecker, 2013). The same number of semilandmarks is placed on the curves and surfaces of every specimen in approximately corresponding locations (either manually or semi-automatically using a template). The specimens are Procrustes superimposed and the semilandmarks are allowed to slide along the curves and surfaces. A Procrustes superimposition standardizes the landmarks by centering the specimens together, scaling them all to the same size, and rotating them into the same orientation. The sliding removes the effects of arbitrary spacing and optimizes the position of the semilandmarks in regards to an average template shape by minimizing either the Procrustes distance or bending energy between the specimen and the average shape (Gunz et al., 2005, Gunz and Mitteroecker, 2013).

4.2.2 Generalized Procrustes Analysis

When landmark coordinates are placed on individual specimens, they are recorded with respect to a defined coordinate axis and the numerical values of their position reflect the orientation and location of each specimen according to those axes. The size of the specimen is also reflected in the coordinate configuration (Slice, 2007). The location, orientation, and size will vary with each specimen. In order to analyze shape differences between specimens, the landmark coordinates of each specimen must be aligned in the same general space and scaled to the same size. A Generalized Procrustes Analysis fixes this

problem by “translating and rotating each specimen to minimize the squared, summed distances between corresponding landmarks and an iteratively computed mean landmark configuration” (Slice, 2007 pg. 263). Each specimen is scaled to the same unit centroid size, which is the square root of the sum of squared distances of each landmark to the centroid (the center point of the landmarks). This places the landmarks of all specimens into a common coordinate system and the differences in landmark coordinate locations reflect differences in shape (Slice, 2007).

4.2.3 Quantifying Asymmetry

To determine how the shape of the modern human endocranum differs between the right and left hemispheres using geometric morphometrics, a mirrored version, referred to as the ‘mirrored endocast’, of each specimen’s complete ‘original’ endocast, and landmark coordinates is created. The topography of the left side of the mirrored endocast is then equivalent to the topography of the right side of the original endocast and vice versa. The placement of surface semilandmarks is done using a template of the surface semilandmarks that is placed on both the original and mirrored endocasts using their respective landmarks and curve semilandmark locations.

In order to avoid creating an artificial midline that may not be biologically accurate, an identical surface semilandmark template is placed on the mirrored version of each specimen’s endocast rather than creating a template with paired semilandmarks placed bilaterally across the mid-sagittal plane. The interhemispheric fissure that separates the two hemispheres of the brain is not always medial nor does it always follow a straight line on the endocranial surface, thus it is not equivalent to the mid-sagittal plane of the skull or endocast (Balzeau and Gilissen, 2010). Therefore, a midline is not determined in this study and the same template is placed on the original and mirrored endocasts of each specimen. This also ensures that each surface semilandmark is representing the same location on each hemisphere in the same way it would be representing the same location on different specimens.

4.3 Data Acquisition and Processing

4.3.1 Virtual Endocast Segmentation

Specimens were downloaded from the ORSA online database in the DICOM (Digital Imaging and Communications in Medicine) file format and imported into the computer program Avizo 7.0. Within Avizo, virtual endocasts were extracted from the CT scans using two- and three-dimensional semi-automated segmentation (Neubauer et al., 2009). Segmentation is an image processing technique used to delineate objects within an image by assigning a label to individual pixels in the image based on certain criteria. As CT scans are gray-scale images, a gray-level thresholding technique was used. First, a minimum and maximum gray-level intensity was defined for bone and every pixel within that range was selected, segmenting the cranium (Figure 4.1a). Next, the three-dimensional segmented cranium was artificially expanded, adding a ~9-pixel thick layer around the cranial surface (Figure 4.1b and c). This closed small foramina and sutures and decreased the amount of manual segmentation needed. The foramen magnum was then manually closed, along with any other remaining open foramina. The internal volume of the cranium was filled and selected to create a three-dimensional virtual endocast (Figure 4.1d and e). Next, the expanded layer of bone was deleted (Figure 4.1f) and the endocast selection was expanded the same amount as the cranium was previously (~9 voxels) (Figure 4.1g and h), so the surface of the virtual endocast matched the endocranial surface of the cranium. Lastly, the endocast was reviewed and corrected manually where the segmentation did not correspond exactly to the bone surface on each CT image slice. A three-dimensional surface model of the endocranial segmentation was then created and exported from the software.

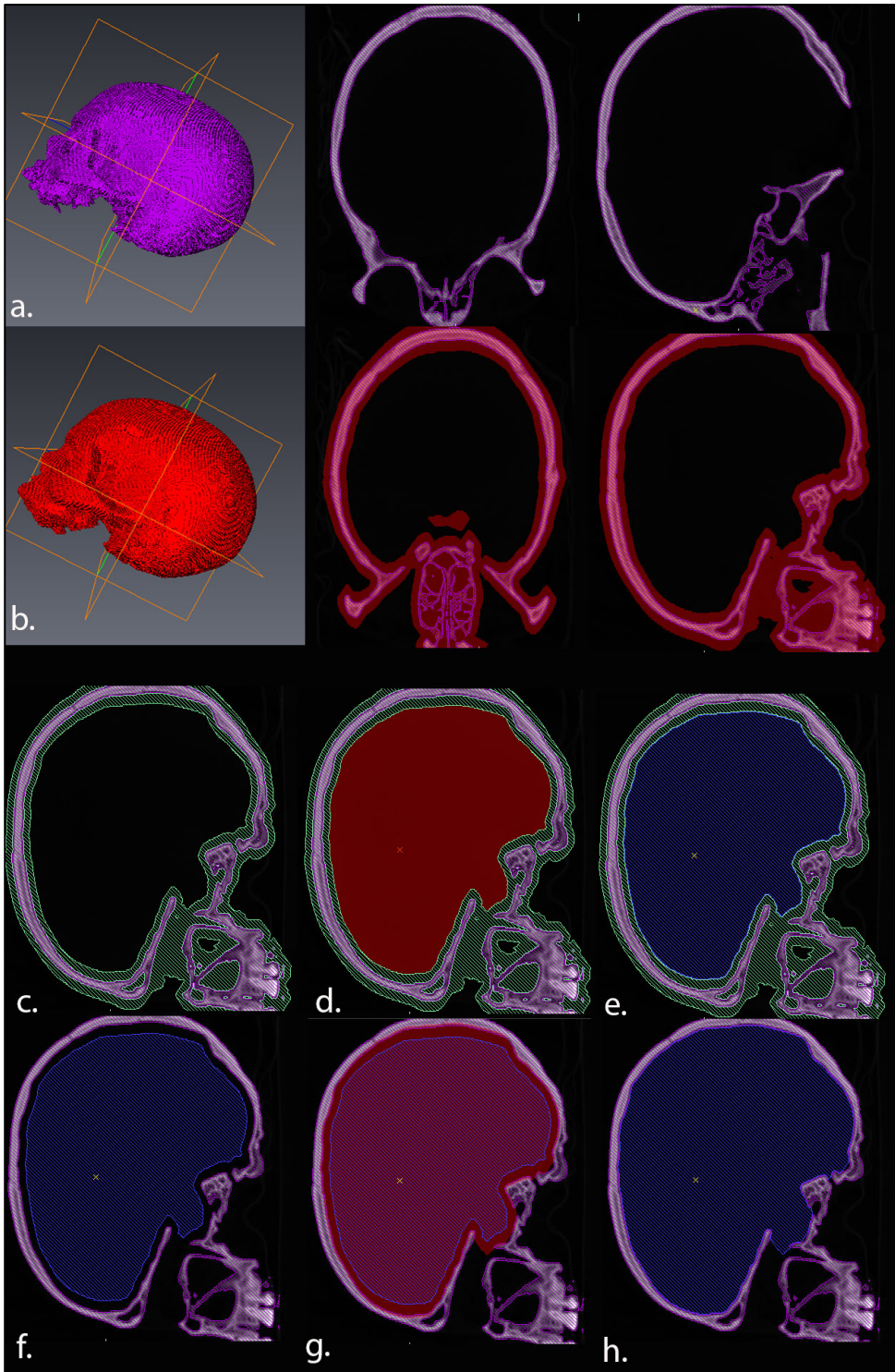


Figure 4.1 Semi-automated method for endocranial segmentation. (a) The gray level intensity for bone is defined and the cranium is segmented. (b and c) The cranial segmentation is expanded and the remaining open foramina are closed. (d and e) The internal volume of the cranium is filled. (f) The expanded cranial segmentation is deleted. (g and h) The endocast segmentation is expanded to meet the cranium and is reviewed and corrected manually where the segmentation does not correspond exactly to the bone surface.

4.3.2 Fixed Landmark and Curve Semilandmark Placement

For each specimen, 29 fixed landmarks (Figure 4.2 and Table 4.1) and 5 curves (Figure 4.3 and Table 4.2) were digitized on bony structures of the endocranial surface (Neubauer et al., 2009). These landmarks were primarily used as reference points for the placement of the surface semilandmarks on and not for the description of endocranial asymmetry. The fixed landmarks and curve outlines were placed in Avizo. Because many of the landmark locations are based on foramina of the cranium, an isosurface (three dimensional surface representation) of the skull was visualized in conjunction with the original endocast to facilitate the correct placement of the landmarks. A clipping plane was used to view the inner surface of the cranium and endocast. To outline the five curves a continuous line of points was placed along each curve. The five curves consisted of the right and left petrous curves, the right and left transverse curves, and the midsagittal curve. The curve outlines were exported from Avizo and resampled to a smaller number of equidistant semilandmarks using the resample.exe program developed by the NYCEP morphometrics group (Reddy et al., 2006). The resample.exe program uses weighted linear interpolation to resample a curvilinear set of semilandmarks into a user-defined number of evenly spaced semilandmarks. After resampling, there were a total of 80 curve semilandmarks representing the 5 curves.

To evaluate landmark precision, the fixed landmarks and curve semilandmarks of one specimen were placed five different times. The error percentage was calculated by comparing the average standard deviation of all landmarks to the average distance between all landmarks. If the error percentage was less than or equal to 3% the accuracy of the landmark placement was accepted (Corner et al., 1992, von Cramon-Taubadel et al., 2007).

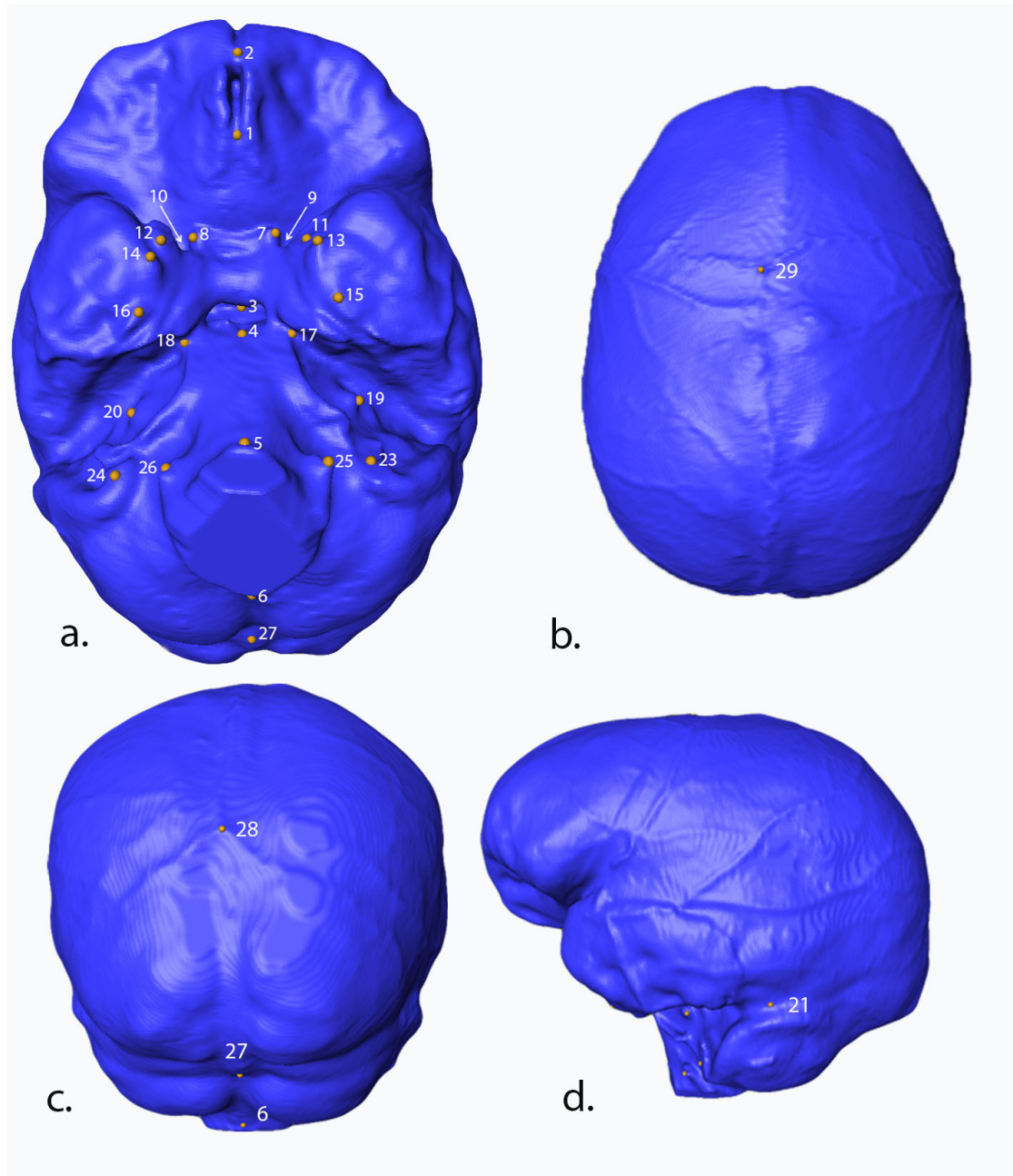


Figure 4.2 Placement of the Fixed Landmarks. (a) Inferior view. (b) Superior view. (c) Posterior view. (d) Left sagittal view.

Table 4.1 Description of the Fixed Landmarks. List of fixed anatomical landmarks placed on the endocranum of each specimen.

#	Name	Description
1	Anterior sphenoid spine	Anterior point of the ethmoidal spine of the sphenoid bone
2	Foramen caecum	Notch anterior to the cribriform plate of ethmoid bone
3	Dorsum sellae	Midpoint of the square portion of bone on the body of the sphenoid posterior to the hypophysial fossa
4	Endosphenobasion	The internal midpoint on the spheno-occipital synchondrosis
5	Basion	Interior midpoint of the anterior margin of the foramen magnum
6	Opisthion	Interior midpoint of the posterior margin of the foramen magnum
7	Anterior clinoid process (left)	Posterior process of the lesser wing of the sphenoid bone
8	Anterior clinoid process (right)	Posterior process of the lesser wing of the sphenoid bone
9	Optic foramen (left)	Opening to the optic canal
10	Optic foramen (right)	Opening to the optic canal
11	Superior orbital fissure (left)	Foramen between the lesser and greater wings of the sphenoid bone
12	Superior orbital fissure (right)	Foramen between the lesser and greater wings of the sphenoid bone
13	Foramen rotundum (left)	Circular foramen in the greater wing of the sphenoid bone
14	Foramen rotundum (left)	Circular foramen in the greater wing of the sphenoid bone
15	Foramen ovale (left)	Foramen in the posterior part of the greater wing of the sphenoid bone
16	Foramen ovale (right)	Foramen in the posterior part of the greater wing of the sphenoid bone
17	Petros apex (left)	Interior anterior tip of the temporal bone
18	Petros apex (right)	Interior anterior tip of the temporal bone
19	Internal acoustic meatus (left)	Canal within the petrous part of the temporal bone
20	Internal acoustic meatus (right)	Canal within the petrous part of the temporal bone
21	Maximum curvature (left)	Maximum curvature point between petrous and transverse curves
22	Maximum curvature (right)	Maximum curvature point between petrous and transverse curves
23	Jugular foramen (left)	Large aperture at the junction of the temporal and occipital bones
24	Jugular foramen (right)	Large aperture at the junction of the temporal and occipital bones
25	Hypoglossic canal (left)	Canal located superior to the occipital condyles
26	Hypoglossic canal (right)	Canal located superior to the occipital condyles
27	Internal occipital protuberance	The intersection of the four divisions of the cruciform eminence
28	Endolambda	Internal point of the intersection of the sagittal and lambdoid sutures
29	Endobregma	Internal point of the intersection of the sagittal and coronal sutures

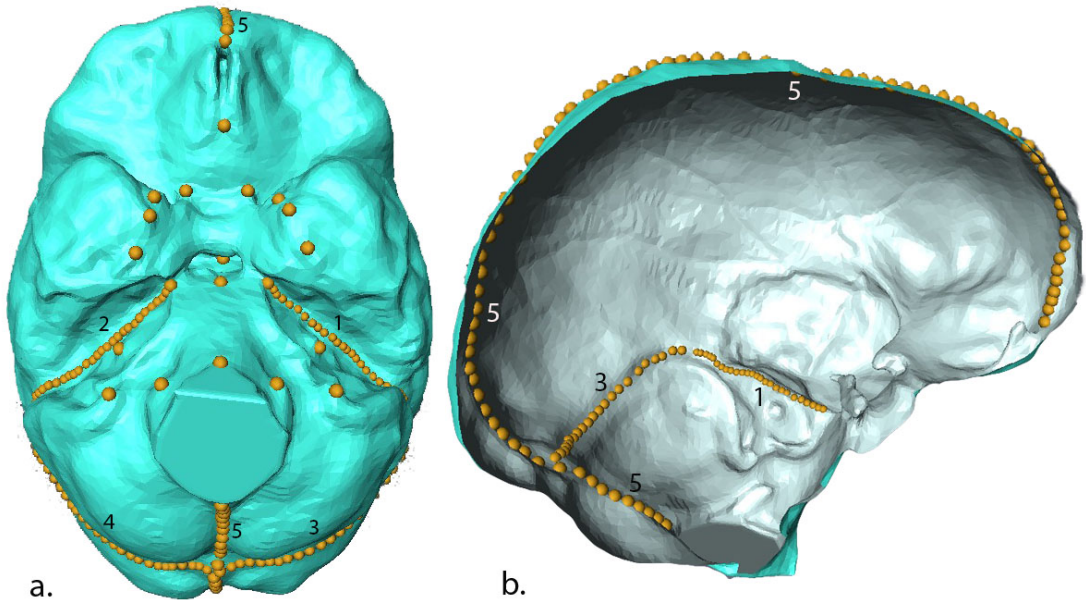


Figure 4.3 Placement of the Curve Outlines. (a) Inferior view. (b) Interior cross section of the right sagittal view.

Table 4.2 Description of the Curves. List of the curves outlined on the endocranial of each specimen.

#	Name	Description
1	Petrosus curve (Left)	Forms the boundary between the middle and the posterior cranial fossa from the petrous apex to the maximum curvature point
2	Petrosus curve (Right)	Forms the boundary between the middle and the posterior cranial fossa from the petrous apex to the maximum curvature point
3	Transverse curve (Left)	Forms the boundary between the posterior cranial fossa and the cranial vault from the maximum curvature point to the internal occipital protuberance
4	Transverse curve (Right)	Forms the boundary between the posterior cranial fossa and the cranial vault from the maximum curvature point to the internal occipital protuberance
5	Midsagittal curve	Follows the sagittal suture and endocranial midline from the opisthion to the foramen caecum

4.3.3 Mirroring the Endocasts and Landmarks

Once the endocast was segmented and the fixed landmarks and curve semilandmarks were placed, the mirrored version of each specimen's data was created using the computer program Meshlab (Cignoni et al., 2008). First, each original endocast model was simplified and saved. The models were simplified, or decimated, using the Quadric Edge Collapse Decimation filter of Meshlab. This

reduced the number of vertices and faces in the three-dimensional model without changing the topography, making it easier for the computer programs used in the next steps to manage. The original endocast models were then reflected, or mirrored, across the x-axis. This created a new, mirrored endocast surface model for each specimen, where the topography that was on the right side of the original endocast is now on the left side, and vice-versa (Figure 4.4). The landmarks and curve landmarks of each specimen were also mirrored by multiplying the x-coordinate value by -1 and switching the order of the paired fixed landmarks and paired curve semilandmarks.

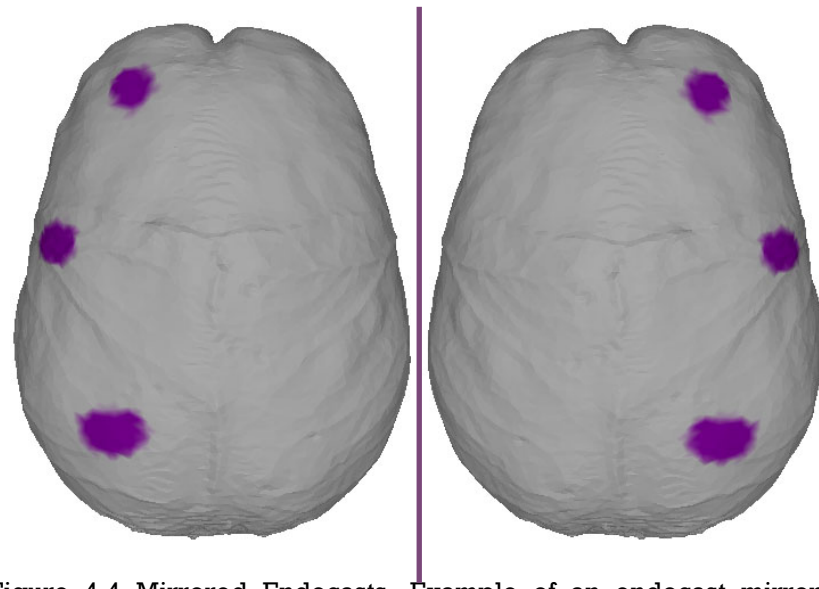


Figure 4.4 Mirrored Endocasts. Example of an endocast mirrored across the x-axis. Purple spots were placed to clearly demonstrate that the shape, location, and topography of the surface are preserved when mirrored.

4.3.4 Surface Semilandmark Placement

The surface semilandmarks were placed on each specimen's original and mirrored endocasts using the package Geomorph within the statistical software R (Adams and Otárola - Castillo, 2013, Adams et al., 2015). A template of 860 roughly equidistant surface semilandmarks was digitized on one specimen's original endocast using the *buildtemplate* function of Geomorph (Figure 4.5). The *buildtemplate* function places a user-defined number (in this case – 860) of surface semilandmarks on the endocranum using an algorithm described in Gunz et al.

(2005) and Mitteroecker and Gunz (2009). The template of surface semilandmarks was then warped to each specimen's original and mirrored endocasts using the *digitsurface* function of the package Geomorph. Based on the location of the fixed landmarks and curve semilandmarks, *digitsurface* placed the same number of surface semilandmarks in the same location as the template on each endocast (Adams et al., 2015, Gunz et al., 2005, Mitteroecker and Gunz, 2009). The *digitsurface* function down samples each surface model, registers the template file with the specimen using a generalized procrustes analysis, and uses a nearest neighbor algorithm to match the location of each endocast's surface semilandmarks with the template's surface semilandmarks (Adams et al., 2015).

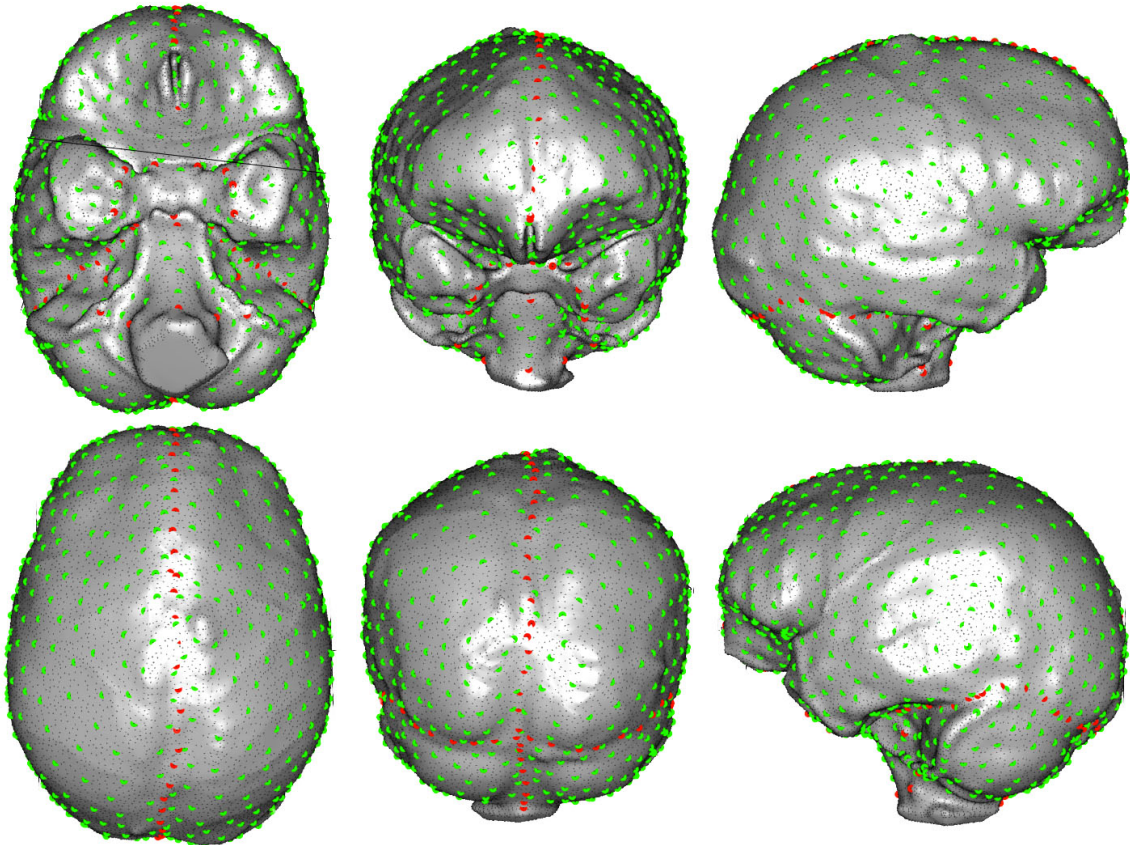


Figure 4.5 Surface Semilandmarks. 860 surface semilandmarks (green) were placed on each specimen's original and mirrored endocasts using the location of the fixed landmarks and curve semilandmarks (red).

4.3.5 Semilandmark Sliding and Generalized Procrustes Analysis

A generalized procrustes analysis was performed using the *gpagen* function of the Geomorph package in R (Adams and Otárola - Castillo, 2013,

Adams et al., 2015). All of the specimens' original and mirrored landmark and semilandmark configurations were superimposed, scaled, and rotated until the corresponding coordinates of all endocasts were aligned as closely as possible. Additionally, in order to optimize their location, the semilandmarks on the curves and surfaces of each endocast were slid along their tangent directions, or planes, by minimizing the Procrustes distance between the template and target specimens (Adams et al., 2015). The curve and surface semilandmarks of each endocast were then fixed and to ensure correct measurement of asymmetry, each specimen's pair of endocasts (original and mirrored) were individually Procrustes aligned to each other using the *gpagen* function.

4.4 Data Analysis

4.4.1 Where Is the Modern Human Endocranum Asymmetric and What Is the Variance at Those Locations?

4.4.1.1 Overall Asymmetry Value (OAV)

The Procrustes distance was measured between each specimen's original and mirrored endocast landmark configurations, producing a value (hereafter referred to as the Overall Asymmetry Value) that describes the overall amount of asymmetry for that specimen (Ventrice, 2011). The Procrustes distance is the square root of the sum of squared distances between all of the corresponding landmarks of two shapes (Webster and Sheets, 2010), in this case between the original and mirrored endocasts of each specimen. The Overall Asymmetry Value revealed which specimens are the most and least asymmetric, as well as the variation in amount of asymmetry.

4.4.1.2 Degree of Asymmetry

Additionally, the Procrustes distance was measured between each corresponding landmark of the original and mirrored endocast pairs to determine which specific landmarks were asymmetric (NOTE: the Procrustes distance was measured between single landmarks for this analysis instead of the whole configuration as in the OAV analysis). The mean and standard deviation of the Procrustes distance between each landmark pair was calculated and used to

describe where and to what degree the modern human endocranum is asymmetric, as well as the variation of those asymmetries. It is important to note, however, that because the left side of the original endocast is identical to the right side of the mirrored endocast and vice versa, the pattern of asymmetry described by the Procrustes distances is the same on both sides and does not show the direction of asymmetry.

4.4.1.3 *Direction of Asymmetry*

In order to determine the direction of asymmetry, the shape differences between the mean shape of the original endocasts and the mean shape of the mirrored endocasts were plotted using the *plotRefToTarget* function of the Geomorph package in R (Adams and Otárola - Castillo, 2013, Adams et al., 2015). The mean shapes of the original and mirrored endocasts were created through the estimation of the average landmark coordinate configuration for each set of endocasts using the *mshape* function of Geomorph. To plot the shape differences, vectors, or lines, were drawn from the landmarks of the mean mirrored endocast to the corresponding landmarks of the mean original endocast. The direction of the vectors illustrated the mean direction of asymmetry.

4.4.2 Is There Sexual Dimorphism in the Modern Human Endocranial Asymmetry Pattern?

To test for sexual dimorphism in the amount of asymmetry, an independent-samples t-test was conducted to compare the Overall Asymmetry Values of male and female endocranial. The t-test results revealed if there was a significant difference between how asymmetric female and male endocasts are. Additionally, individual independent-samples t-tests were performed on the Procrustes distance values for each landmark pair between the original and mirrored endocast configurations to determine if there was any sexual dimorphism in the pattern of asymmetry.

Chapter 5

5 Results

5.1 Landmark Precision

The evaluation of landmark precision indicated that the average standard deviation of landmarks was equal to 1.01% of the average distance between all landmarks. The accuracy of the landmark placement was accepted because it does not exceed a 3% error percentage (von Cramon-Taubadel et al., 2007, Corner et al., 1992).

5.2 Where Is the Modern Human Endocranum Asymmetric and What Is the Variance at Those Locations?

5.2.1 Overall Asymmetry Value

The Overall Asymmetry Value, which describes the overall amount of endocranial asymmetry for each specimen, was determined by calculating the Procrustes distance between each specimen's original and mirrored endocasts. The OAV quantifies the total amount of asymmetry, but does not indicate the locations or directions of the asymmetries. The OAV for each specimen is listed in Table 5.1 and plotted in Figure 5.1. Twenty-two of the 28 specimens were within one standard deviation of the mean Overall Asymmetry Value (Mean OAV = 0.03025364, SD = ± 0.0078129). The most and least asymmetric specimens were identified as the specimens with the highest and lowest OAV, respectively (Figure 5.2). Interestingly, the specimen with the highest overall amount of asymmetry, morton1329, displayed a reversed petalial pattern of asymmetry (Toga and Thompson, 2003), where the left frontal and right occipital lobes were larger and extended further out than the opposite lobes (Figure 5.2).

Table 5.1 Overall Asymmetry Values. The Overall Asymmetry Value quantifies the total amount of asymmetry for each specimen.

Specimen #	Specimen Name	OAV	Specimen #	Specimen Name	OAV
1	morton1103	0.02606266	15	morton51	0.03164386
2	morton1188	0.02350483	16	morton547	0.03747899
3	morton1192	0.02382872	17	morton631	0.03460899
4	morton1306	0.01828403	18	morton645	0.02439577
5	morton1319	0.0293212	19	morton646	0.02908276
6	morton1329	0.05256988	20	morton762	0.02427614
7	morton1486	0.04030145	21	morton772	0.04711485
8	morton1973	0.03689703	22	morton778	0.03674337
9	morton25	0.02981766	23	morton787	0.02140206
10	morton413	0.02681366	24	morton808	0.03596461
11	morton422	0.02730648	25	morton901	0.01972761
12	morton432	0.02736541	26	morton902	0.02516127
13	morton434	0.02955656	27	morton913	0.03087365
14	morton451	0.02755974	28	morton915	0.0294387

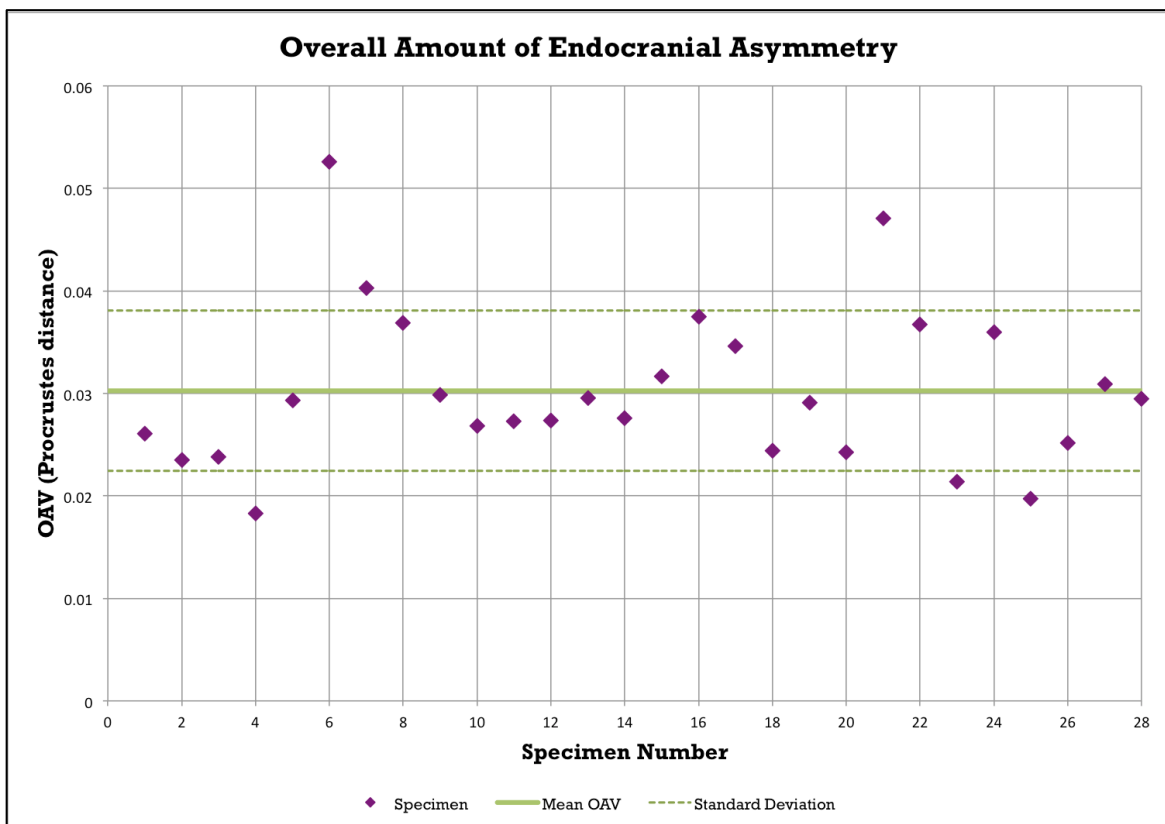


Figure 5.1 Overall Amount of Endocranial Asymmetry. Plot of the Overall Asymmetry Value for each specimen. Mean OAV = 0.03025364, standard deviation = ± 0.0078129 .

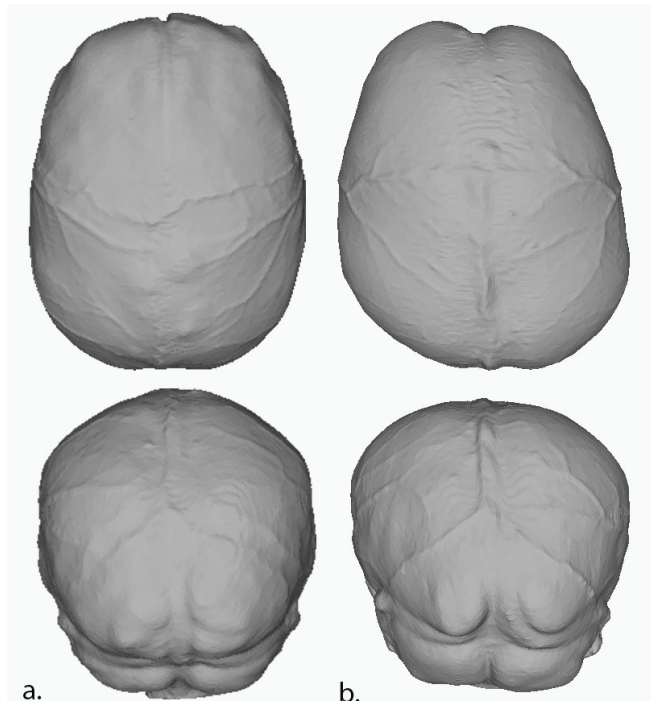


Figure 5.2 The Least and Most Asymmetric Specimens. (a) Superior and posterior views of the specimen with the lowest amount of asymmetry, morton1306. (b) Superior and posterior views of the specimen with the highest amount of asymmetry, morton1329.

5.2.2 Degree of Asymmetry

The Procrustes distance was measured between the corresponding landmark pairs of each specimen's original and mirrored endocast landmark configurations. The mean Procrustes distance for each landmark is shown in Figures 5.3a-5.8a and Figure 5.10. The landmarks of the mean original endocast shape were plotted on a 3D model of the mean original endocast shape. The color of each landmark indicates the mean Procrustes distance of that landmark. During the generalized Procrustes superimposition the specimens' coordinates were all scaled to the same centroid size to allow for the analysis of shape with the effect of size removed. Because of this step, the Procrustes distances do not refer to a distance on a millimeter scale. Instead the Procrustes distances are used to describe the degree of asymmetry at each landmark. The larger the Procrustes distance is between the corresponding landmarks on the original and mirrored endocasts, the more asymmetric that landmark is; the smaller the Procrustes distance, the less asymmetric it is.

The landmarks and their mean Procrustes distances have been plotted twice, once with all of the landmarks (Figures 5.6a-5.8a) (fixed landmarks, curve semilandmarks, and surface semilandmarks) and once with just the surface semilandmarks (Figures 5.3a-5.5a). The fixed landmarks and curve semilandmarks were placed by hand using features of the skull, primarily to serve as reference points for the automatic placement of the surface semilandmarks before sliding. As a result, the asymmetry of these landmarks describes the asymmetry of those specific features of the skull (e.g. the mid-sagittal sulcus and the transverse sinus), and not the endocranum. Additionally, many of these landmarks are much more asymmetric than the surface semilandmarks and make it difficult to view the more subtle degree differences of the surface semilandmarks. By separately plotting just the surface semilandmarks and their mean Procrustes distance we can more easily see the pattern of endocranial asymmetry.

To view the amount of variation in the degree of asymmetry at each landmark, the standard deviation of each landmark's mean Procrustes distance has also been plotted on the mean original endocast shape (Figure 5.9) as well as in Figure 5.10. The standard deviations have also been plotted twice, once with all landmarks (Figure 5.9b) and once with only surface semilandmarks (Figure 5.9a).

5.2.2.1 Surface Semilandmark Degree of Asymmetry

The areas of the endocranum with the highest degree of asymmetry were the superior, lateral regions of the frontal lobes, the lateral, posterior regions of the occipital lobes, the superior, lateral regions of the cerebellum, and the anterior regions of the cerebellum. The inferior and superior edges of the temporal lobes also showed asymmetry, along with the anterior temporal poles. The anterior edge of the orbitofrontal area also showed asymmetry, although the inferior orbitofrontal did not. The parietal lobes, the superior midline, and the inferior midline showed little to no asymmetry. The areas with the highest degree of asymmetry were also approximately the same as the areas with the largest standard deviations.

5.2.2.2 Fixed Landmark and Curve Semilandmark Degree of Asymmetry

The intersection of the midsagittal and transverse curves showed the highest degree of asymmetry overall, as well as the largest standard deviation. The midsagittal curve was the most asymmetric at the posterior of the endocast, but as it wrapped around anteriorly it decreased in degree of asymmetry. The transverse curves also decreased in asymmetry as they wrapped anteriorly. The petrous curves had an intermediate degree of asymmetry. The fixed landmarks with the highest degree of asymmetry were located at the jugular foramen and the hypoglossic canal. All of the fixed landmarks and the petrous curves had small standard deviations. The midsagittal curve and the transverse curves had very large standard deviations at their intersections, but the standard deviations decreased as they wrapped anteriorly.

5.2.3 Direction of Asymmetry

The direction of asymmetry at each landmark was determined by plotting the shape differences between the mean shape of the original endocasts and the mean shape of the mirrored endocasts. Vectors were drawn from the landmark coordinates of the mean mirrored endocast to the corresponding landmarks of the mean original endocast. The vectors for each surface semilandmark are shown in Figures 5.3-5.5b and the vectors for each fixed landmark and curve semilandmark are shown in Figures 5.6-5.8b. To make sure the direction of the vectors was clearly visible, each vector was multiplied by 15. The direction of the vectors indicates the direction of asymmetry and the length of the vectors is indicative of the degree of asymmetry.

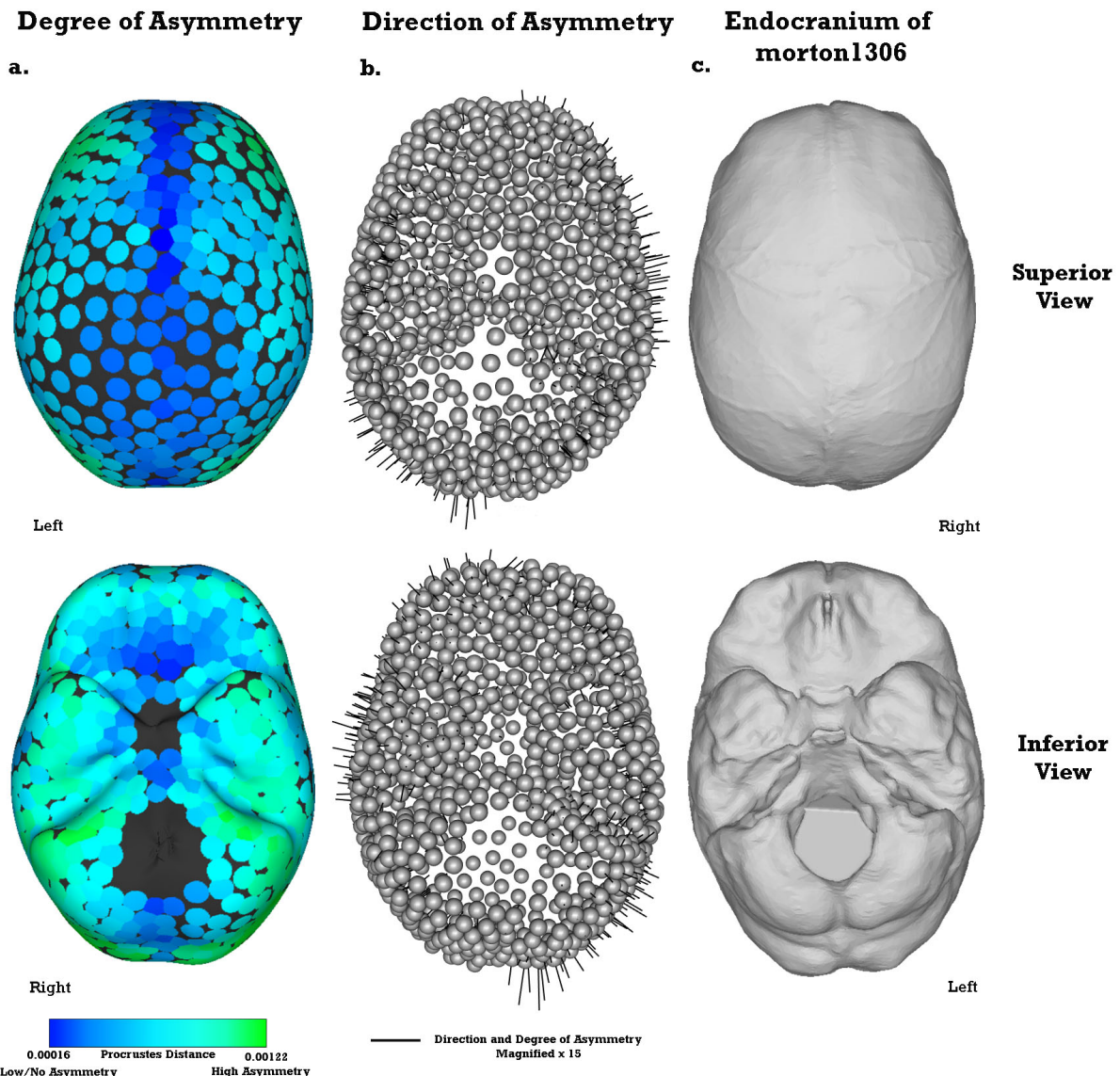
5.2.3.1 Surface Semilandmark Direction of Asymmetry

The results showed a clear petalial pattern of asymmetry. The asymmetric area in the frontal region of the endocranum protrudes more anteriorly, laterally, and superiorly in the right hemisphere than the left. The asymmetric areas in the occipital lobes and superior, posterior cerebellum protrude more posteriorly and laterally in the left hemisphere than the right. The anterior region of asymmetry of the cerebellum is also a leftward asymmetry. There is no leftward asymmetry within the frontal, parietal, or temporal lobes. The rightward frontal

asymmetry extends posteriorly to include the anterior parietal region and the right temporal lobe. The orbitofrontal region hangs lower in the right hemisphere than the left. The temporal pole also protrudes more anteriorly in the right hemisphere. There are two semilandmarks located where the temporal lobe joins the frontal lobe that indicate a leftward asymmetry.

5.2.3.2 Fixed Landmark and Curve Semilandmark Direction of Asymmetry

The midsagittal curve appears to follow a diagonal path, favoring the posterior right hemisphere, but shifting leftward at the anterior tip of the endocranum. The endolambda, however, occurs on the left side. The transverse curve is lower on the left side of the endocranum than the right. The petrous curve protrudes more anteriorly on the left hemisphere than the right. The fixed landmarks with the highest degree of asymmetry, the jugular foramen and hypoglossic canal landmarks, both have an anterior leftward asymmetry.



NOTE: Direction of asymmetry is not indicated in (a).

Figure 5.3 Superior and Inferior Views of the Pattern of Endocranial Asymmetry (Surface Semilandmarks Only). (a) Degree of Asymmetry. The surface semilandmarks are plotted on a 3-D model of the mean original endocast shape and colored to indicate the mean degree of asymmetry at that landmark. (b). Direction of Asymmetry. Vectors are drawn between the mean mirrored endocast's surface semilandmarks to the mean original endocast's surface semilandmarks and plotted on each landmark. The direction of the vectors indicates the direction of asymmetry at that landmark. (c). The endocranum of morton1306. An example of the least asymmetric specimen's endocast for comparison.

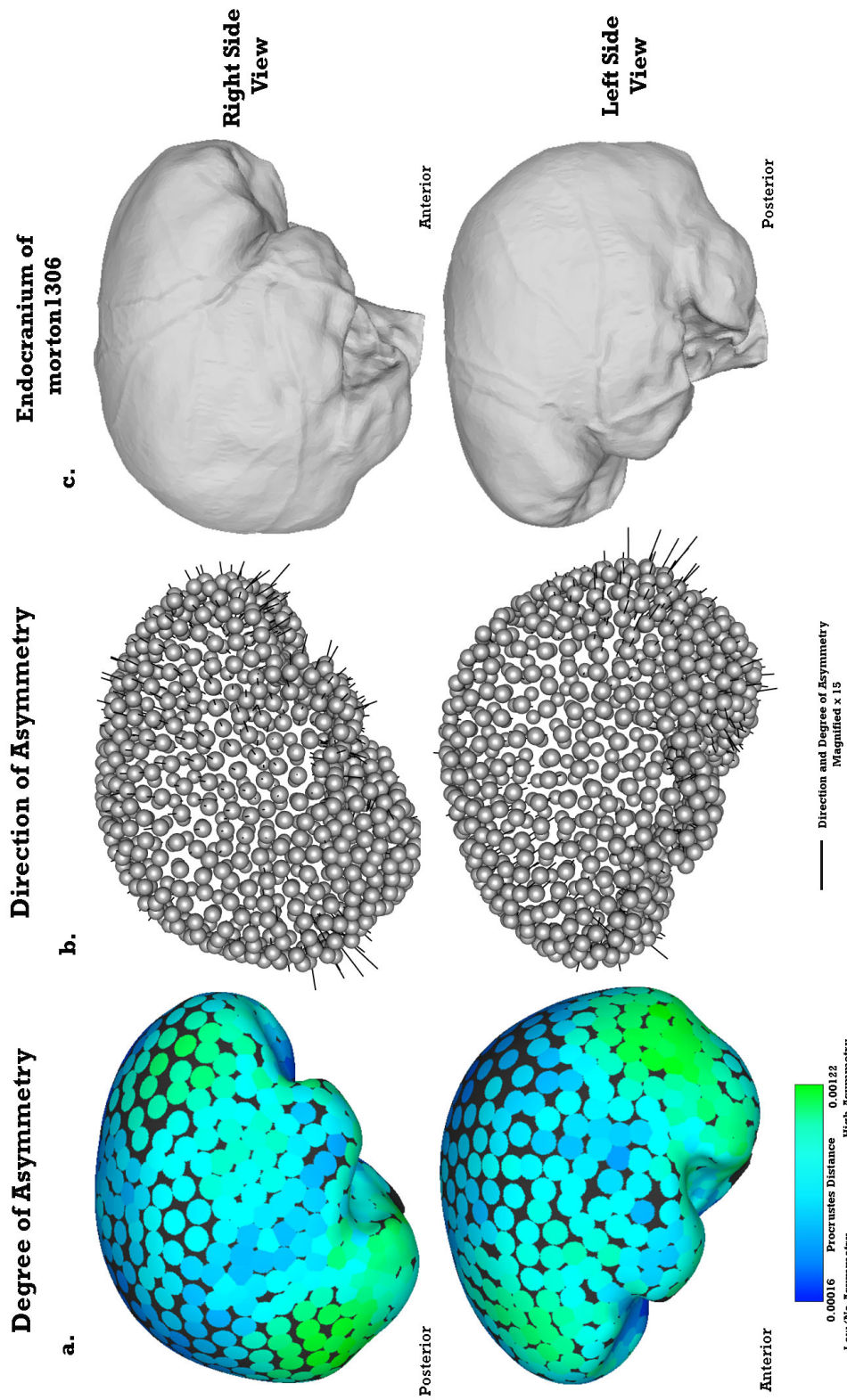
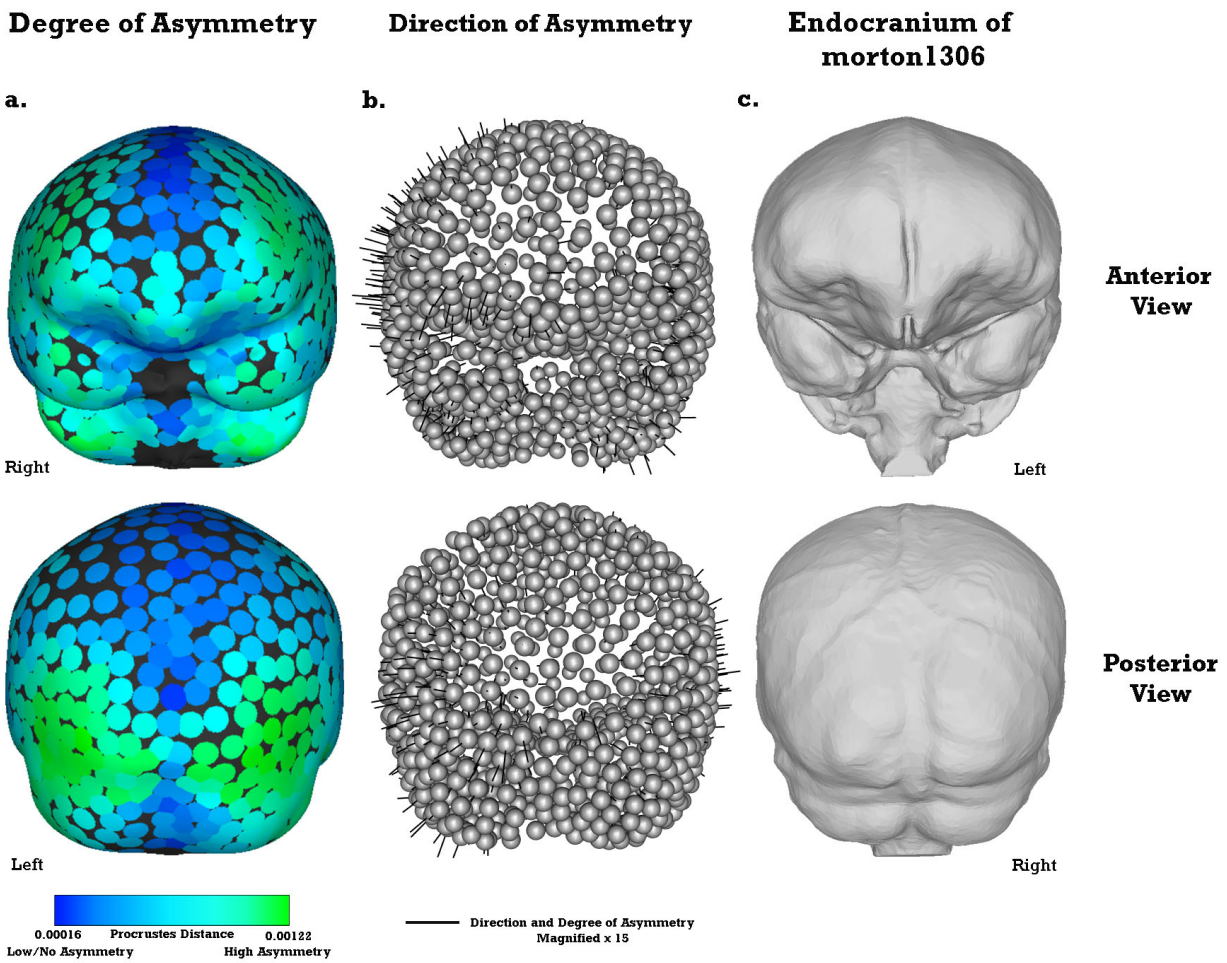


Figure 5.4 Left and Right Side Views of the Pattern of Endocranial Asymmetry (Surface Semilandmarks Only). (a) Degree of Asymmetry. The surface semilandmarks are plotted on a 3-D model of the mean original endocast shape and colored to indicate the mean degree of asymmetry at that landmark. (b) Direction of Asymmetry. Vectors are drawn between the mean mirrored endocast's surface semilandmarks to the mean original endocast's surface semilandmarks and plotted on each landmark. The direction of the vectors indicates the direction of asymmetry at that landmark. (c) The endocranum of morton1306. An example of the least asymmetric specimen's endocast for comparison.



NOTE: Direction of asymmetry is not indicated in (a).

Figure 5.5 Anterior and Posterior Views of the Pattern of Endocranial Asymmetry (Surface Semilandmarks Only). (a) Degree of Asymmetry. The surface semilandmarks are plotted on a 3-D model of the mean original endocast shape and colored to indicate the mean degree of asymmetry at that landmark. (b). Direction of Asymmetry. Vectors are drawn between the mean mirrored endocast's surface semilandmarks to the mean original endocast's surface semilandmarks and plotted on each landmark. The direction of the vectors indicates the direction of asymmetry at that landmark. (c). The endocranum of morton1306. An example of the least asymmetric specimen's endocast for comparison.

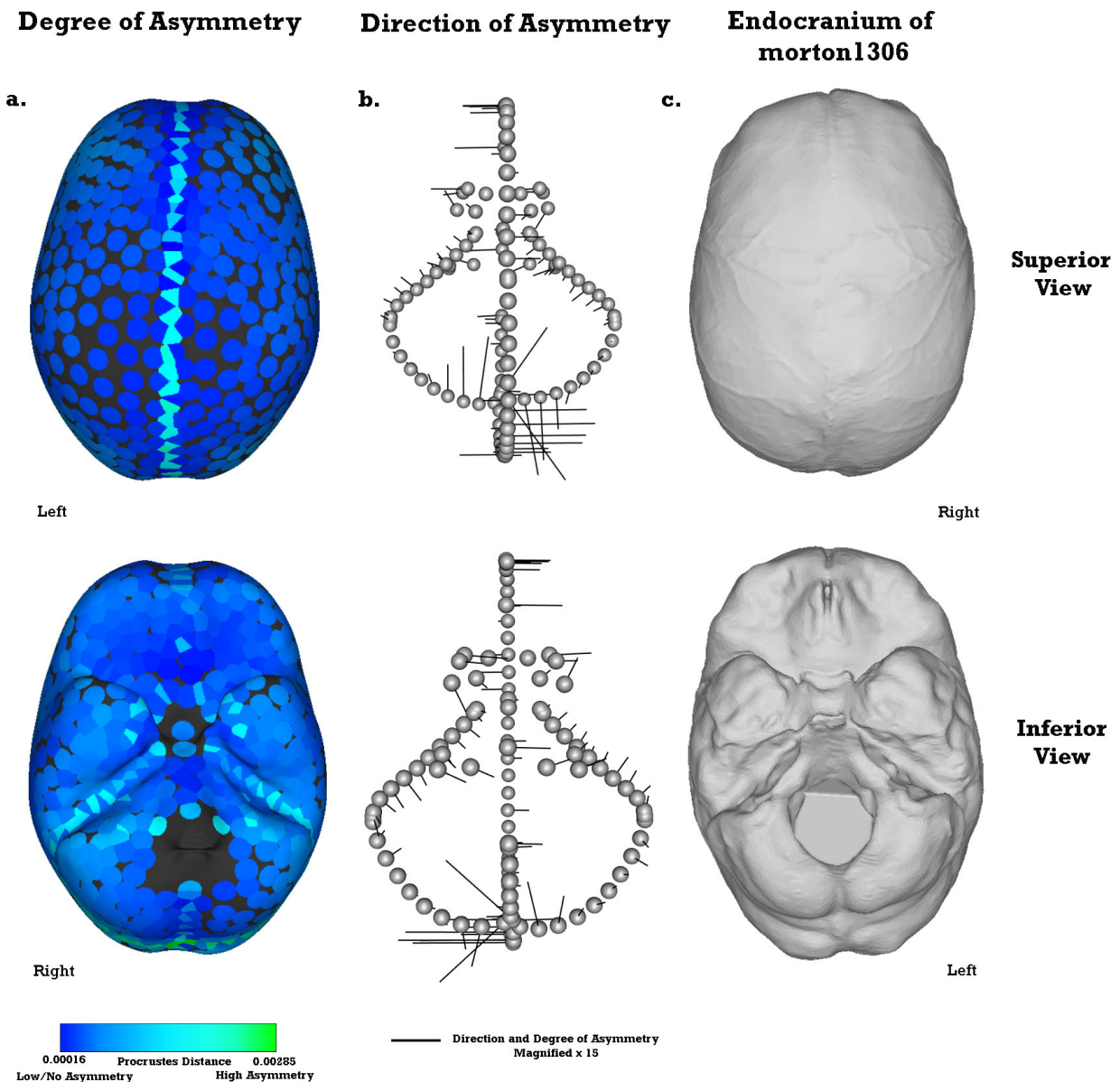


Figure 5.6 Superior and Inferior Views of the Pattern of Endocranial Asymmetry (All Landmarks). (a) Degree of Asymmetry. All landmarks are plotted on a 3-D model of the mean original endocast shape and colored to indicate the mean degree of asymmetry at that landmark. (b). Direction of Asymmetry. Vectors are drawn between the mean mirrored endocast's landmarks to the mean original endocast's landmarks and plotted on each landmark. The direction of the vectors indicates the direction of asymmetry at that landmark. (c). The endocranum of morton1306. An example of the least asymmetric specimen's endocast for comparison.

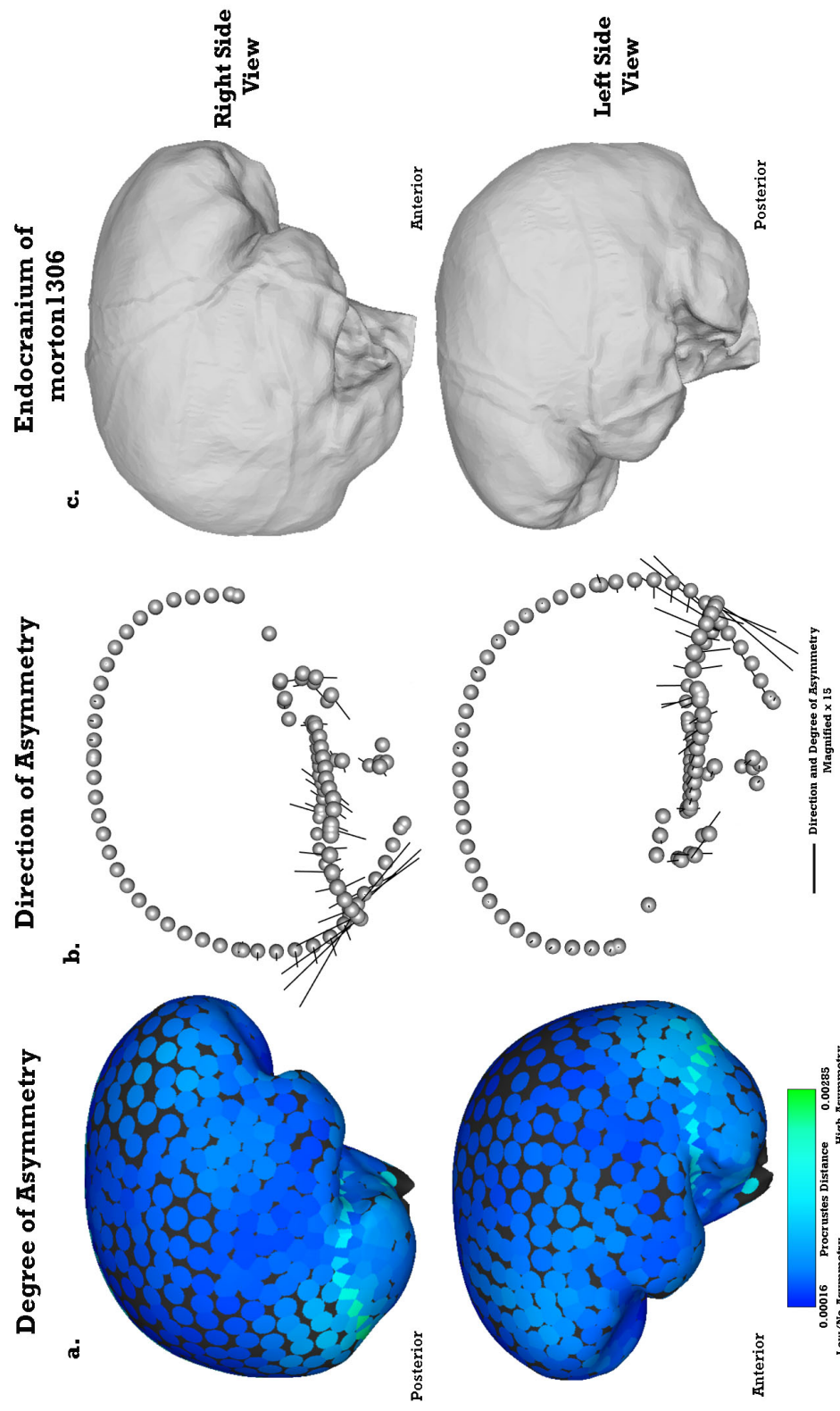
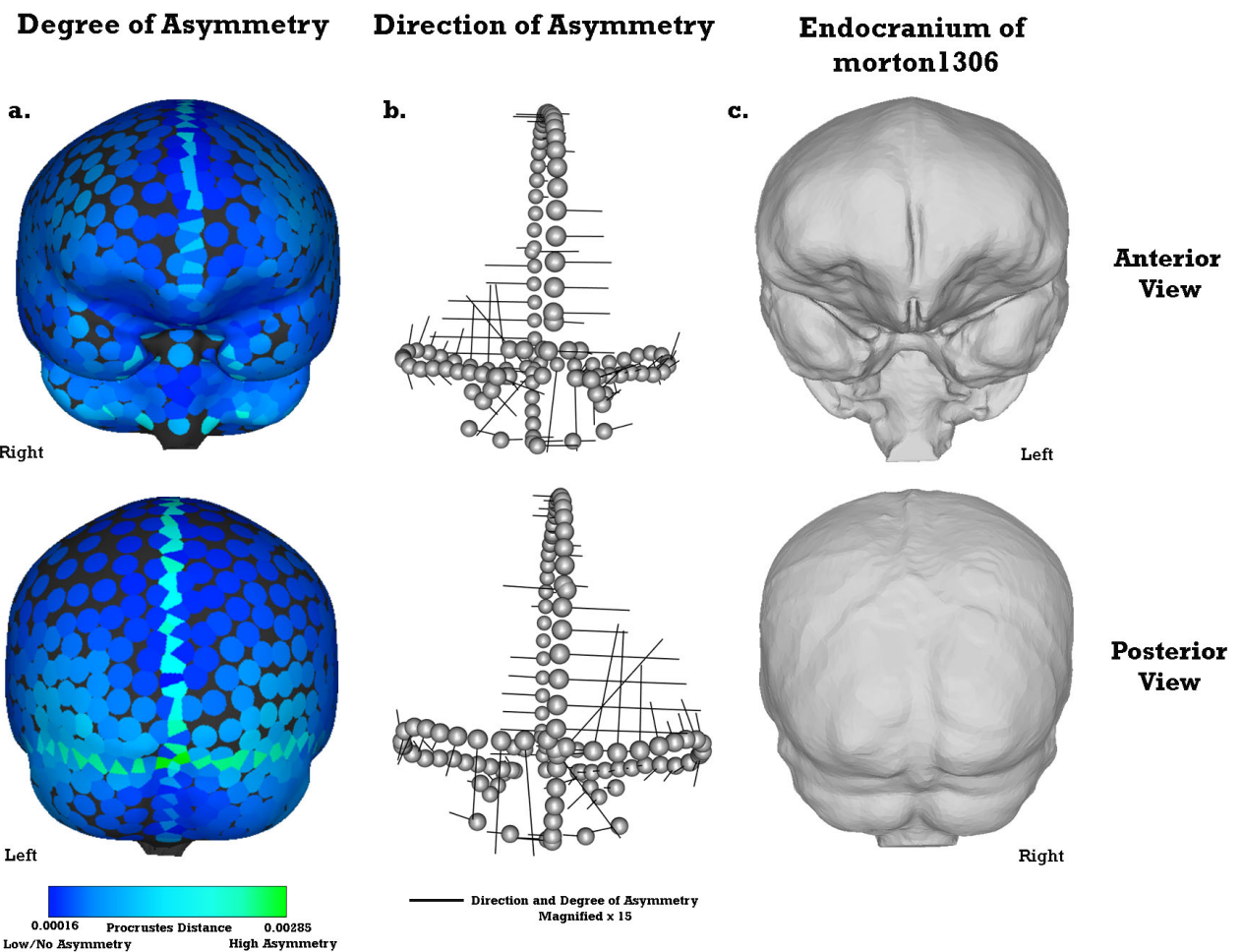


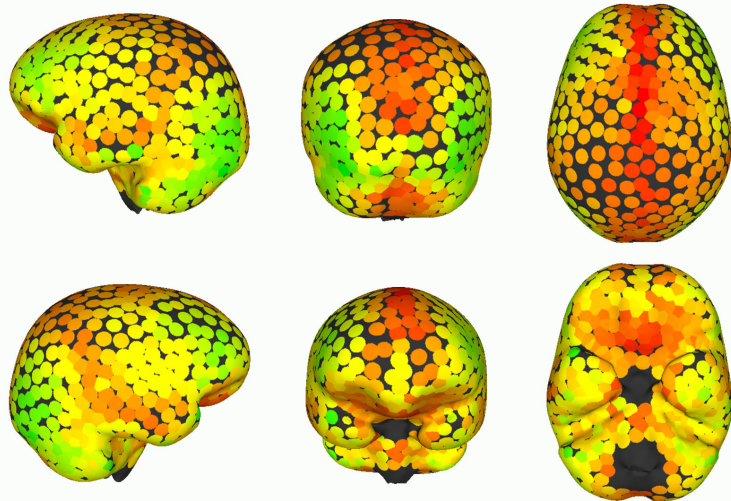
Figure 5.7 Left and Right Side Views of the Pattern of Endocranial Asymmetry (All Landmarks). (a) Degree of Asymmetry. All landmarks are plotted on a 3-D model of the mean original endocast shape and colored to indicate the mean degree of asymmetry at that landmark. (b). Direction of Asymmetry. Vectors are drawn between the mean mirrored endocast's landmarks to the mean original endocast's landmarks and plotted on each landmark. The direction of the vectors indicates the direction of asymmetry at that landmark. (c). The endocranum of morton1306. An example of the least asymmetric specimen's endocast for comparison.



NOTE: Direction of asymmetry is not indicated in (a).

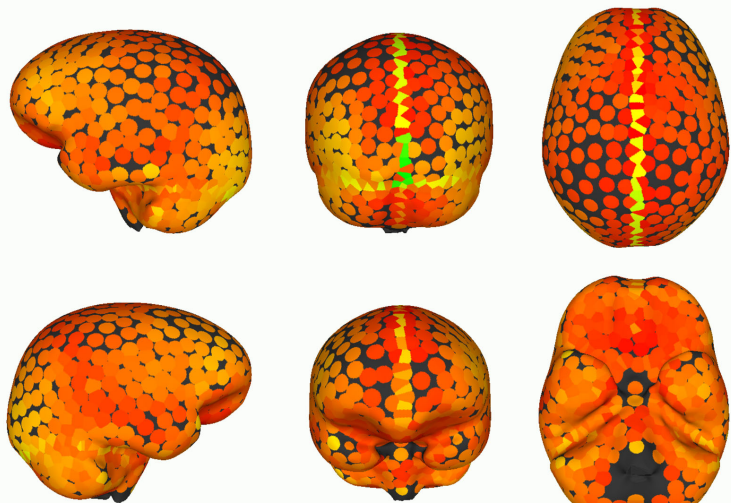
Figure 5.8 Anterior and Posterior Views of the Pattern of Endocranial Asymmetry (All Landmarks).
 (a) Degree of Asymmetry. All landmarks are plotted on a 3-D model of the mean original endocast shape and colored to indicate the mean degree of asymmetry at that landmark. (b). Direction of Asymmetry. Vectors are drawn between the mean mirrored endocast's landmarks to the mean original endocast's landmarks and plotted on each landmark. The direction of the vectors indicates the direction of asymmetry at that landmark. (c). The endocranum of morton1306. An example of the least asymmetric specimen's endocast for comparison.

**Standard Deviation of the
Mean Degree of Asymmetry
of Each Landmark**



a. **Surface
Semilandmarks**

0 Standard Deviation 0.00103
No Variation High Variation



b. **All Landmarks**

0 Standard Deviation 0.00217
No Variation High Variation

Figure 5.9 Standard Deviation of the Mean Degree of Asymmetry of Each Landmark. (a) Standard deviation of the surface semilandmarks plotted on the mean original endocast shape. (b). Standard deviation of all of the landmarks (fixed, curve semilandmarks, and surface semilandmarks) plotted on the mean original endocast shape.

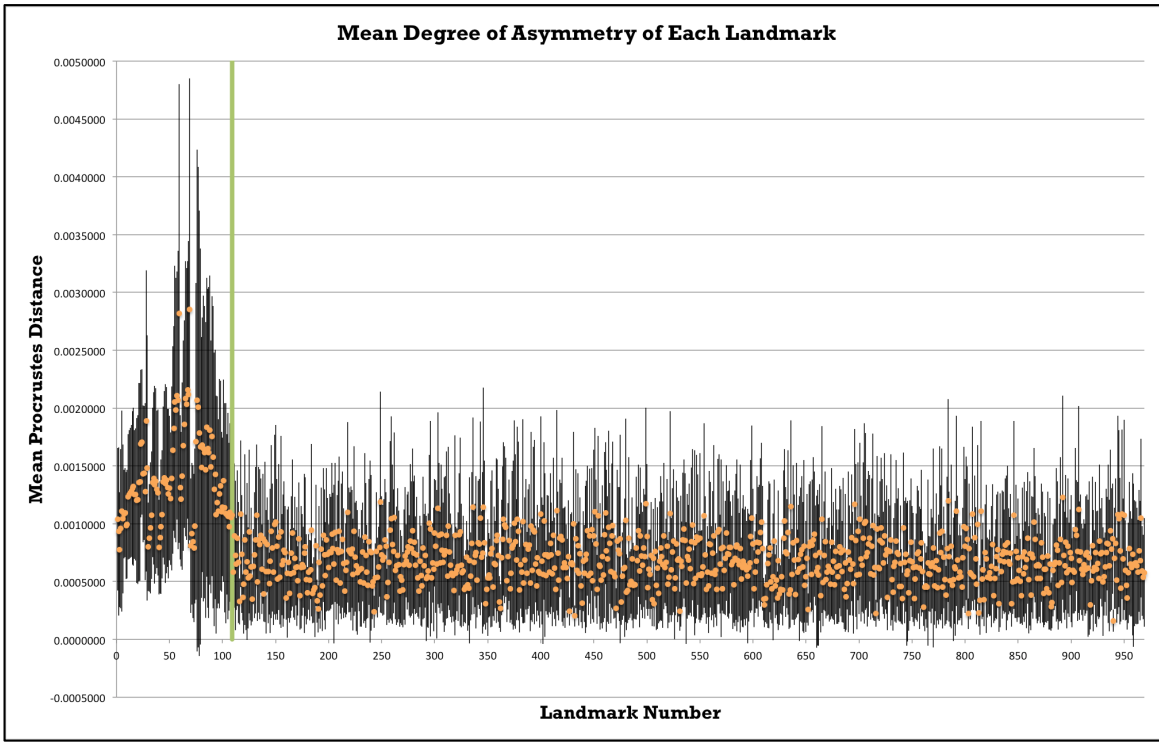


Figure 5.10 Plot of the Mean Degree of Asymmetry and Standard Deviation at Each Landmark. The orange points represent the mean Procrustes distance of each landmark and the black lines show the standard deviation of the mean. The points to the left of the green line are the fixed landmarks and curve semilandmarks. The points to the right of the green line are the surface semilandmarks.

5.3 Is There Sexual Dimorphism in the Modern Human Endocranial Asymmetry Pattern?

An independent-samples t-test was conducted to compare the Overall Asymmetry Values of male and female endocranial to test for sexual dimorphism in the amount of asymmetry (Figure 5.11). There was not a significant difference in the Overall Asymmetry Values between male (mean = 0.029728, SD = 0.00806633) and female (mean = 0.03101001, SD = 0.00777691) specimens; $t(25.965) = 0.5052$, $p = 0.6177$. This indicates that there is no difference in the overall amount of asymmetry between males and females. Independent samples t-tests were also run on each landmark to determine if there was a significant difference between the male and female specimens in the pattern of endocranial asymmetry. 29 of the 969 landmarks showed a significant difference between the male and female specimens ($p < 0.05$). The 29 landmarks with p-values less than 0.05 are plotted on the mean original endocast shape in red next to the mean degree of asymmetry at each landmark of the female and male specimens (Figure 5.12). There are two

clusters of significant landmarks on both the right and left parietals. This suggests that the degree of asymmetry of the top of the parietals is significantly different between the male and female specimens.

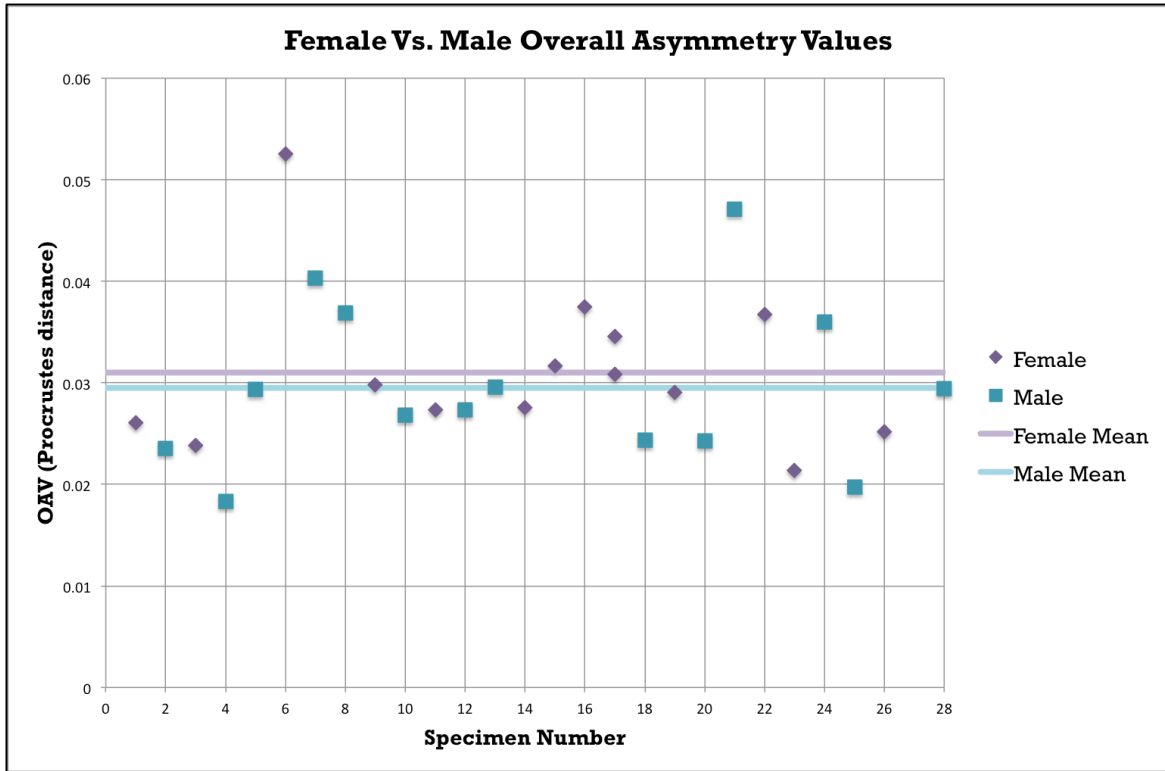


Figure 5.11 Plot of the Female and Male Overall Asymmetry Values and Means.

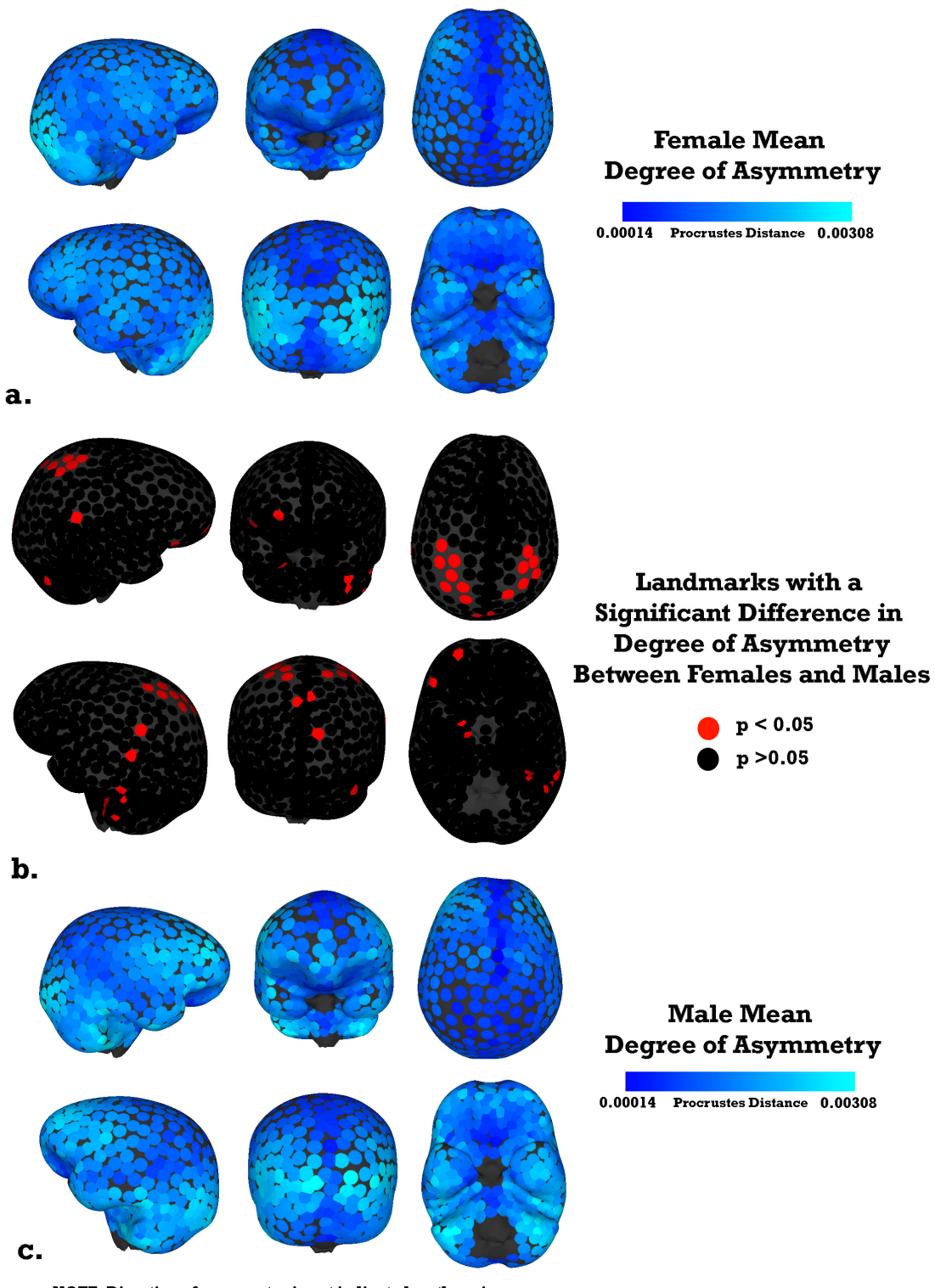


Figure 5.12 Landmarks with a Significant Difference in Degree of Asymmetry between Females and Males. (a) Mean degree of asymmetry of the female specimens. (b) Landmarks with a significant difference in degree of asymmetry between female and male specimens ($p < 0.05$) are plotted in red. (c) Mean degree of asymmetry of the male specimens.

Chapter 6

6 Discussion

This discussion chapter will be split into several sections; the first two will address the two questions and corresponding hypotheses introduced in Chapter Three. The pertaining results will be analyzed and compared to the literature presented in Chapter two. The remaining sections will discuss the brain–endocast relationship, limitations of the study, and suggestions for further research.

6.1 Where Is the Modern Human Endocranum Asymmetric and What Is the Variance at Those Locations?

For each specimen an Overall Asymmetry Value was calculated that described the total amount of asymmetry for the endocranum. There was a fair amount of variation in the OAV, but two specimens (one male, one female) appeared to be outliers. Both were on the high end of the OAVs, indicating that they had a much higher than average amount of asymmetry. There were no clear outliers on the lower end of the OAV range. All specimens had some degree of asymmetry; even on the least asymmetric specimen, morton1306, a rightward frontal petalia is visible (Figure 5.2a). The specimen with the highest OAV, morton1329, displayed an extreme reversed petalial pattern of asymmetry (Figure 5.2b). The left frontal and right occipital lobes were larger and protruded out further than the lobes of the opposite hemisphere. According to brain asymmetry research, it is likely that this individual was not right handed (Bear et al., 1986, Galaburda et al., 1978, LeMay, 1976, LeMay et al., 1982, LeMay and Kido, 1978). Additionally, morton1329 was female, in line with the notion that females are more likely to exhibit reversed or reduced petalia asymmetries (Bear et al., 1986).

The degree and direction of asymmetry results replicated many of the findings of previous research on endocranial asymmetry. Before discussing additional findings of my research, I will first address the two hypotheses for this question presented in Chapter Three.

6.1.1 Hypothesis 1: The modern human endocranum will show a petalial pattern of asymmetry with the right frontal and left occipital lobes protruding out more than the opposite hemisphere.

This hypothesis was not rejected. The average endocranial shape did show a petalial pattern of asymmetry with the right frontal and left occipital lobes protruding out more than the opposite hemisphere. Specifically, the results indicated that the frontal lobe extended more anteriorly, laterally, and superiorly in the right hemisphere than the left, while the occipital lobe extended more posteriorly, laterally, and inferiorly in the left hemisphere than the right. The superior and inferior extensions were not reported previously in the literature, until now research has primarily focused on the width and anterior-posterior distribution of the two hemispheres. Additionally, the frontal petalia was found to encompass the right temporal lobe and extend as far back as the posterior end of the Sylvian fissure (lateral sulcus), including an anterior portion of the right parietal region. The occipital petalia extended below the transverse sulcus to include a superior portion of the left posterior cerebellum. The transverse and midsagittal curves also supported a right frontal/left occipital petalial pattern. These curves also had the highest degree of asymmetry overall. On average, the transverse curve was found to be much lower on the left hemisphere of the skull. As the transverse sinus typically delineates the inferior extension of the occipital lobe, this supports the existence of a larger and lower left occipital. The midsagittal curve was found to typically run diagonally from a more rightward position starting where it intersects the transverse curve to a more leftward position at the anterior end of the endocast.

However, the results did demonstrate that this particular petalial pattern of asymmetry was not the case for every endocranum, as was seen in the specimen with the highest amount of asymmetry, morton1329. Additionally, the standard deviations for the mean degree of asymmetry at each landmark were highest for the landmarks involved in the petalial pattern of asymmetry, for both the surface semilandmarks and the curve semilandmarks. This suggests that while on average the modern human endocranum has a right frontal and left occipital petalial asymmetry pattern, the degree and direction of this pattern is not entirely

consistent. As seen in brain asymmetry research, the degree and direction of the petalias can vary depending on sex and handedness (although the relationships are not obligate) and it is likely the same case for these results.

The petalial pattern of asymmetry found does support previous research conducted on endocranial petalia asymmetry (Balzeau et al., 2012a, Balzeau et al., 2012b, Fournier et al., 2011b, Holloway and de la Coste-Lareymondie, 1982, Holloway et al., 2004a, LeMay, 1976, LeMay and Kido, 1978). The findings of this study are particularly relevant to the Balzeau et al. (2012b) study on surface area asymmetries within the genus *Homo*. Similar to my results, in addition to the larger right frontal lobe, they also found that the parieto-temporal region was larger in the right hemisphere. The diagonal position of the midsagittal curve suggests the presence of the Yakovlevian anticlockwise torque, the distortion of the midline by the occipital lobe (LeMay, 1976, Toga and Thompson, 2003).

6.1.2 Hypothesis 2: The area of Broca's cap will be larger on the right side of the endocranum, but more globular in appearance on the left side.

This hypothesis was not rejected, but the results found were not entirely supportive. The average endocranial shape did show a rightward asymmetry of the Broca's cap region, but it did not indicate a more globular shape in the left hemisphere. Two surface semilandmarks located at the anterior tip of the Sylvian fissure, where the frontal and temporal lobes are joined, showed a small leftward asymmetry, however, these landmarks reveal more about the Sylvian fissure than Broca's cap. It is not clear if Broca's cap is actually larger on the right hemisphere, or simply more laterally located. The frontal lobe may extend so much more laterally overall in the right than the left that any smaller regions of asymmetry are overridden. Any asymmetry of Broca's cap might be smaller than the shape difference between the two frontal lobes. Moreover, the asymmetry of Broca's cap may be relative to the surface of the frontal lobe, independent of the petalial pattern of asymmetry, and if so, might not be visible when the shape of the endocranial surface is examined globally. It is also possible that the landmarks placed were not dense enough to pick up more subtle asymmetries within the region of Broca's cap.

The results of this study do support the results reported in Balzeau et al. (2014). As the first study to qualitatively measure Broca's cap, Balzeau et al. (2014) found that the cap was larger in the right hemisphere, but more clearly defined in the left. This finding contradicts previously published literature on Broca's cap, in which all have claimed to find a larger Broca's cap in the left hemisphere (e.g. Falk, 1983, Holloway, 1983a, Holloway, 1995, Holloway et al., 2004a, Tobias, 1987). The visual and qualitative nature of these studies suggests that the researchers were likely influenced by global asymmetries or overall endocranial shape, creating an illusion of a larger left Broca's cap. The stark contrast between the results of the quantitative versus the qualitative studies suggests that visual descriptions and identifications, while useful in some cases, may not be very reliable. The results of this study show the value of validating qualitative claims through quantitative measurements.

6.1.3 Additional Regions of Asymmetry

Another large area of asymmetry was visible in the cerebellar region of the endocranum. The results showed a leftward asymmetry of the anterior cerebellum. The petrous curve, which delineates the anterior/superior boundary of the cerebellum, was also located more anteriorly on the left side of the endocranum than the right side. This endocranial asymmetry matches a leftward anterior asymmetry visible on the cerebellar tissue of modern human brains, but does not replicate the corresponding rightward asymmetry of the posterior cerebellum (Kitchell et al., 2013). The cerebellum is particularly interesting because it has been found to play a role in coordinated motor tasks (Nair et al., 2003, Nitschke et al., 1996). Additionally, cerebellar asymmetries are significantly associated with handedness in some non-human primates (Catalupo et al., 2008, Phillips and Hopkins, 2007). The cerebellum is infrequently discussed in the context of human evolution, but it appears that an asymmetry of this area is readily visible on a modern human endocast. If the cerebellar asymmetry of the modern human brain is found to correlate with handedness, the cerebellar region of the endocranum may be useful in estimating the handedness of fossil hominins.

Although it may be considered part of the right frontal petalia asymmetry, regions within the temporal lobe also displayed a rightward asymmetry. The anterior temporal pole extended more anteriorly and the region corresponding to the inferior temporal gyrus extended more laterally in the right hemisphere than the left. The middle gyrus of the temporal lobe was not very asymmetric. The fact that almost all areas of asymmetry were either located within the rightward frontal petalia or the leftward occipital petalia suggests that the methodology used in this research is unfortunately very sensitive to the petalial pattern of asymmetry. The degree of asymmetry caused by the petalias is too large to allow for the quantification of smaller topographical surface asymmetries. The lack of additional, more localized regions of asymmetry in the results of this study does not mean they are not there. Further research needs to be done on smaller regions of the endocranum independent of the global asymmetries.

6.2 Is There Sexual Dimorphism in the Modern Human Endocranial Asymmetry Pattern?

As in the last section, before addressing additional findings I will first address the hypothesis presented in Chapter three.

6.2.1 Hypothesis 3: Male specimens will have a higher degree of global petalia asymmetry compared to the female specimens.

This hypothesis was rejected. The results of an independent samples t-test conducted to compare the Overall Asymmetry Values of the male and female specimens showed no significant difference. Male specimens did not have a higher amount of asymmetry on average than female specimens. The standard deviation of the male values was larger than the standard deviation of the female values, however. This suggests there was more variance in the amount of asymmetry for male specimens than female specimens, although the difference in the standard deviations was small. Additionally, the results of independent samples t-tests on the degree of asymmetry of each landmark showed no difference in the petalial pattern of asymmetry between the male and female specimens (Figure 5.12). These results contradict the brain asymmetry research

by Bear et al. (1986), where the brains of male modern humans showed a greater degree of right frontal and left occipital petalias than the females. It is possible that the sample used in this study was too small to get a clear view of sexual dimorphism patterns. This study had 28 specimens (14 males and 14 females), which is almost half the amount of subjects measured in Bear et al. (1986) ($n= 66$, 30 males and 36 females).

There was a significant difference between male and female specimens in the asymmetry of 29 of the landmarks. 13 of those landmarks were clustered in an area of the superior parietal region of both hemispheres. This suggests that there is a significant difference between males and females in the degree of asymmetry of the superior parietal. It appears that females have a higher degree of asymmetry in this region than males. In line with these results, Good et al. (2001) used voxel based morphometrics to examine brain asymmetry and the effects of sex on brain structure and found that females had a greater amount of grey and white matter in several regions within the parietal lobes. Watkins et al. (2001) did not measure sex differences, but they also examined structural brain asymmetries using voxel based morphometrics and found a leftward asymmetry of several areas within the parietal lobes. Although asymmetries of the parietal region of the endocranum have not been discussed previously, the results of this study fit with the limited previous research on parietal brain asymmetry.

6.3 Limitations

A limitation of this study is the small sample size. It is possible that the specimens used are not a good representation of the entire population of modern humans or that there were too few specimens to show accurate trends of the pattern of endocranial asymmetry. The addition of more specimens would allow for a better sense of the overall asymmetry at the population level and would indicate if the results shown here are accurate or an artifact of the specific specimens measured. A limitation of the methodology used is the inability to get an actual metric measurement of the degree of asymmetry. Because each specimen was individually scaled to the centroid size, the numbers used to determine degree of asymmetry only indicated a relative difference in degree.

This allowed for a representation of the patterns of asymmetry but did not allow for a direct metric measurement of the shape differences. Additionally, because the original and mirrored endocasts were aligned as a whole, the results were greatly influenced by global asymmetries. This is not inherently bad or inaccurate, but it meant that the large petalias overrode any smaller, subtler, topographic surface asymmetries.

6.4 Does The Endocranial Asymmetry of Modern Humans Accurately Correspond to the Brain Asymmetry of Modern Humans?

The answer to this question is very complicated. According to the results of this research, it does appear that the average pattern of asymmetry of the modern human endocranum matches some of the areas of asymmetry found on the average modern human brain. The petalias, as was already known, are very visible on the endocranial surface. The anterior cerebellar asymmetry of the brain can also be seen on an endocast. However, smaller asymmetric regions, such as those found within the motor cortex of the brain, were not visible. It is possible that these asymmetries do appear on the endocranial surface, but they would be small topographical changes that may not show up due to the nature of the methods. Additionally, it is likely that the petalias are the result of several smaller regions of asymmetry within the brain. For example, many of the areas of asymmetry found within the frontal lobe of the brain are internal and not located on the surface (Good et al., 2001, Hervé et al., 2006, Kitchell et al., 2013, Luders et al., 2004, Watkins et al., 2001). It is the sum of these asymmetries that leads to a large shift in the entire hemisphere. This shift is very visible on the endocranial surface when examined using geometric morphometrics with surface semilandmarks, but the smaller individual asymmetries are not.

6.5 Suggestions for Further Research

Further research needs to be done on smaller areas of the endocranum independent of the whole surface. The global petalias make it very difficult to capture subtle differences in the topography of the endocranial surface between

hemispheres. Differences may exist, but the lateral shift of the entire hemisphere overrides any smaller changes when the endocranum is studied as a whole.

Additionally, research comparing the brain and endocranum of the same subjects would help determine quantitatively if the degree and direction of the asymmetry visible on the endocranum is identical to the degree and direction of asymmetry visible on the brain. We do not know if the degree and direction is always the same as the brain, or if the degree of asymmetry is more or less severe than the degree of asymmetry of the brain. Bruner et al. (2015) has shown the spatial relationship between some cerebral and cranial elements to be very weak. It may be that very asymmetric frontal and occipital lobes of the endocranum are due to very asymmetric lobes of the brain, or it could be that slightly asymmetric lobes of the brain lead to slightly more asymmetric tissues around the brain, which lead to very asymmetric lobes of the endocranum. Further investigation into the brain-endocast relationship will help answer these questions and hopefully give us more answers about our hominin ancestors' brains.

Chapter 7

7 Conclusion

Hominin brain evolution is a topic of great interest in paleoanthropology and details of the evolutionary process are typically inferred from endocasts. However, very little research has been done to quantifiably establish the relationship between an endocast and its corresponding brain. The questions investigated in this dissertation were developed to begin quantifying this relationship, using asymmetry of the endocranial surface. As the modern human brain has been shown to be structurally asymmetric, the results of this study allowed for a direct comparison of this characteristic between the two surfaces. This research was unique in that it quantified asymmetry of the *entire* endocranial surface using new geometric morphometric techniques. Previous research on endocranial asymmetry has either been purely qualitative or focused on anterior-posterior or lateral asymmetries using fixed landmarks.

The results of this dissertation research indicate that the well-known petalial pattern of asymmetry extends beyond the frontal lobe to include the right temporal and anterior parietal regions. In addition to an anterior-posterior and lateral asymmetry, the petalias also differ in their superior-inferior distribution. A rightward asymmetry of Broca's area was found, contradicting previous qualitative reports. A leftward asymmetry of the anterior cerebellum was also found, as well as a rightward asymmetry of the inferior temporal gyrus and the temporal pole. There was no significant difference in amount of asymmetry or degree of petalial asymmetry between the male and female specimens. However, there was a significant difference between sexes in the degree of asymmetry of the superior parietal region.

The results also suggest that the average pattern of asymmetry of the modern human endocranum does match some of the areas of asymmetry found on the average modern human brain. However, smaller asymmetric regions were not visible due to the methodology's sensitivity to the petalial asymmetry. Further

research should be done to quantify smaller topographic asymmetries of the endocranial surface independent of the global endocranial shape.

References

- ADAMS, D. C., COLLYER, M. L. & SHERRATT, E. 2015. *geomorph*: Software for geometric morphometric analyses. 2.1.x ed.
- ADAMS, D. C. & OTÁROLA - CASTILLO, E. 2013. *geomorph*: an R package for the collection and analysis of geometric morphometric shape data. *Methods in Ecology and Evolution*, 4, 393-399.
- ADAMS, D. C., ROHLF, F. J. & SLICE, D. E. 2004. Geometric morphometrics: ten years of progress following the 'revolution'. *Italian Journal of Zoology*, 71, 5-16.
- ALBANESE, E., MERLO, A., ALBANESE, A. & GOMEZ, E. 1989. Anterior speech region: asymmetry and weight-surface correlation. *Archives of neurology*, 46, 307-310.
- ALLEN, J. S., BRUSS, J. & DAMASIO, H. 2006. Looking for the lunate sulcus: a magnetic resonance imaging study in modern humans. *The Anatomical Record Part A: Discoveries in Molecular, Cellular, and Evolutionary Biology*, 288, 867-876.
- ANTHONY, R. 1913. L'encéphale de l'homme fossile de la Quina. *Bulletins et Mémoires de la Société d'anthropologie de Paris*, 4, 117-195.
- BALZEAU, A. & GILISSEN, E. 2010. Endocranial shape asymmetries in *Pan paniscus*, *Pan troglodytes* and *Gorilla gorilla* assessed via skull based landmark analysis. *Journal of human evolution*, 59, 54-69.
- BALZEAU, A., GILISSEN, E. & GRIMAUD-HERVÉ, D. 2012a. Shared pattern of endocranial shape asymmetries among great apes, anatomically modern humans, and fossil hominins. *PLoS One*, 7, e29581.
- BALZEAU, A., GILISSEN, E., HOLLOWAY, R. L., PRIMA, S. & GRIMAUD-HERVÉ, D. 2014. Variations in size, shape and asymmetries of the third frontal convolution in hominids: Paleoneurological implications for hominin evolution and the origin of language. *Journal of human evolution*.
- BALZEAU, A., HOLLOWAY, R. L. & GRIMAUD-HERVÉ, D. 2012b. Variations and asymmetries in regional brain surface in the genus *Homo*. *Journal of human evolution*, 62, 696-706.
- BARRICK, T. R., MACKAY, C. E., PRIMA, S., MAES, F., VANDERMEULEN, D., CROW, T. J. & ROBERTS, N. 2005. Automatic analysis of cerebral asymmetry: an exploratory study of the relationship between brain torque and planum temporale asymmetry. *Neuroimage*, 24, 678-691.
- BEAR, D., SCHIFF, D., SAVER, J., GREENBERG, M. & FREEMAN, R. 1986. Quantitative analysis of cerebral asymmetries: Fronto-occipital correlation, sexual dimorphism and association with handedness. *Archives of Neurology*, 43, 598-603.
- BIENVENU, T., GUY, F., COUDYZER, W., GILISSEN, E., ROUALDÈS, G., VIGNAUD, P. & BRUNET, M. 2011. Assessing endocranial variations in great apes and humans using 3D data from virtual endocasts. *American journal of physical anthropology*, 145, 231-246.

- BOOKSTEIN, F. L. 1997. *Morphometric tools for landmark data: geometry and biology*, Cambridge University Press.
- BOULE, M. & ANTHONY, R. 1911. L'encéphale de l'homme fossile de la Chapelleaux-Saints. *L'anthropologie*, 22.
- BROADFIELD, D. C., HOLLOWAY, R. L., MOWBRAY, K., SILVERS, A., YUAN, M. S. & MARQUEZ, S. 2001. Endocast of Sambungmacan 3 (Sm 3): a new Homo erectus from Indonesia. *The Anatomical Record*, 262, 369-379.
- BROCA, P. 1861. Perte de la parole, ramollissement chronique et destruction partielle du lobe antérieur gauche du cerveau. *Bull Soc Anthropol*, 2, 235-238.
- BRUNER, E. 2004. Geometric morphometrics and paleoneurology: brain shape evolution in the genus *Homo*. *Journal of Human Evolution*, 47, 279-303.
- BRUNER, E. 2007. Cranial shape and size variation in human evolution: structural and functional perspectives. *Child's Nervous System*, 23, 1357-1365.
- BRUNER, E. 2010. Morphological differences in the parietal lobes within the human genus. *Current Anthropology*, 51, S77-S88.
- BRUNER, E., AMANO, H., DE LA CUÉTARA, J. M. & OGIHARA, N. 2015. The brain and the braincase: a spatial analysis on the midsagittal profile in adult humans. *Journal of Anatomy*, 227, 268-276.
- BRUNER, E., DE LA CUÉTARA, J. M., MASTERS, M., AMANO, H. & OGIHARA, N. 2014. Functional craniology and brain evolution: from paleontology to biomedicine. *Frontiers in neuroanatomy*, 8.
- BRUNER, E. & HOLLOWAY, R. L. 2010. A bivariate approach to the widening of the frontal lobes in the genus *Homo*. *Journal of Human Evolution*, 58, 138-146.
- BRUNER, E., MANZI, G. & ARSUAGA, J. L. 2003. Encephalization and allometric trajectories in the genus *Homo*: evidence from the Neandertal and modern lineages. *Proceedings of the National Academy of Sciences*, 100, 15335-15340.
- CANTALUPO, C., FREEMAN, H., RODES, W. & HOPKINS, W. 2008. Handedness for tool use correlates with cerebellar asymmetries in chimpanzees (*Pan troglodytes*). *Behavioral neuroscience*, 122, 191.
- CARLSON, K. J., STOUT, D., JASHASHVILI, T., DE RUITER, D. J., TAFFOREAU, P., CARLSON, K. & BERGER, L. R. 2011. The endocast of MH1, *Australopithecus sediba*. *Science*, 333, 1402-1407.
- CIGNONI, P., CALLIERI, M., CORSINI, M., DELLEPIANE, M., GANOVELLI, F. & RANZUGLIA, G. MeshLab: an Open-Source Mesh Processing Tool. Eurographics Italian Chapter Conference, 2008. 129-136.
- CONNOLLY, C. J. 1950. *External morphology of the primate brain*, CC Thomas.
- CONSORTIUM, T. C. S. A. A. 2005. Initial sequence of the chimpanzee genome and comparison with the human genome. *Nature*, 437, 69-87.
- CORNER, B. D., LELE, S. & RICHTSMEIER, J. T. 1992. Measuring precision of three-dimensional landmark data. *Medicine, Baltimore*, 1500, 21205.
- DE SOUSA, A. A., SHERWOOD, C. C., MOHLBERG, H., AMUNTS, K., SCHLEICHER, A., MACLEOD, C. E., HOF, P. R., FRAHM, H. & ZILLES, K. 2010. Hominoid visual brain structure volumes and the position of the lunate sulcus. *Journal of human evolution*, 58, 281-292.

- DEANER, R. O., ISLER, K., BURKART, J. & VAN SCHAIK, C. 2007. Overall brain size, and not encephalization quotient, best predicts cognitive ability across non-human primates. *Brain, Behavior and Evolution*, 70, 115-124.
- DORSAINT-PIERRE, R., PENHUNE, V. B., WATKINS, K. E., NEELIN, P., LERCH, J. P., BOUFFARD, M. & ZATORRE, R. J. 2006. Asymmetries of the planum temporale and Heschl's gyrus: relationship to language lateralization. *Brain*, 129, 1164-1176.
- EDINGER, T. 1929. Die fossilen Gehirne.
- EDINGER, T. 1937. *Capitosaurus-gaumen und unterkiefer aus süddeutschem haupt-buntsandstein*.
- EDINGER, T. 1948a. Evolution of the horse brain. *Geological Society of America Memoirs*, 25, 1-178.
- EDINGER, T. 1948b. Paleoneurology versus comparative brain anatomy. *Stereotactic and Functional Neurosurgery*, 9, 5-24.
- EDINGER, T. 1974. Paleoneurology 1804-1966: an annotated bibliography. *Advances in anatomy, embryology, and cell biology*, 49, 3-258.
- ELTON, S., BISHOP, L. C. & WOOD, B. 2001. Comparative context of Plio-Pleistocene hominin brain evolution. *Journal of Human Evolution*, 41, 1-27.
- FALK, D. 1980. A reanalysis of the South African australopithecine natural endocasts. *American Journal of Physical Anthropology*, 53, 525-539.
- FALK, D. 1983. Cerebral cortices of East African early hominids. *Science*, 221, 1072-1074.
- FALK, D. 1985. Hadar AL 162-28 endocast as evidence that brain enlargement preceded cortical reorganization in hominid evolution.
- FALK, D. 2009. The natural endocast of Taung (*Australopithecus africanus*): Insights from the unpublished papers of Raymond Arthur Dart. *American journal of physical anthropology*, 140, 49-65.
- FALK, D. 2012. Hominin paleoneurology: where are we now? In: HOFMAN, M. & FALK, D. (eds.) *Evolution of the primate brain: from neuron to behavior*.
- FALK, D., HILDEBOLD, C., CHEVERUD, J., KOHN, L. A., FIGIEL, G. & VANNIER, M. 1991. Human cortical asymmetries determined with 3D MR technology. *Journal of neuroscience methods*, 39, 185-191.
- FALK, D., HILDEBOLD, C., SMITH, K., MORWOOD, M. J., SUTIKNA, T., BROWN, P., JATMIKO, SAPTOMO, E. W., BRUNSDEN, B. & PRIOR, F. 2005. The Brain of LB1, *Homo floresiensis*. *Science*, 308, 242-245.
- FALK, D., REDMOND, J. C., GUYER, J., CONROY, C., RECHEIS, W., WEBER, G. W. & SEIDLER, H. 2000. Early hominid brain evolution: a new look at old endocasts. *Journal of Human Evolution*, 38, 695-717.
- FALZI, G., PERRONE, P. & VIGNOLO, L. A. 1982. Right-left asymmetry in anterior speech region. *Archives of Neurology*, 39, 239.
- FOUNDAS, A. L., EURE, K. F., LUEVANO, L. F. & WEINBERGER, D. R. 1998. MRI asymmetries of Broca's area: the pars triangularis and pars opercularis. *Brain and language*, 64, 282-296.
- FOUNDAS, A. L., LEONARD, C. M., GILMORE, R., FENNELL, E. & HEILMAN, K. M. 1994. Planum temporale asymmetry and language dominance. *Neuropsychologia*, 32, 1225-1231.

- FOUNDAS, A. L., LEONARD, C. M., GILMORE, R. L., FENNELL, E. B. & HEILMAN, K. M. 1996. Pars triangularis asymmetry and language dominance. *Proceedings of the National Academy of Sciences*, 93, 719-722.
- FOUNDAS, A. L., LEONARD, C. M. & HANNA-PLADDY, B. 2002. Variability in the anatomy of the planum temporale and posterior ascending ramus: Do right- and left handers differ? *Brain and Language*, 83, 403-424.
- FOUNDAS, A. L., WEISBERG, A., BROWNING, C. A. & WEINBERGER, D. R. 2001. Morphology of the frontal operculum: a volumetric magnetic resonance imaging study of the pars triangularis. *Journal of Neuroimaging*, 11, 153-159.
- FOURNIER, M., COMBÈS, B., ROBERTS, N., BRAGA, J. & PRIMA, S. Mapping the distance between the brain and the inner surface of the skull and their global asymmetries. SPIE Medical Imaging, 2011a. International Society for Optics and Photonics, 79620Y-79620Y-7.
- FOURNIER, M., COMBÈS, B., ROBERTS, N., KELLER, S., CROW, T. J., HOPKINS, W. D. & PRIMA, S. Surface-based method to evaluate global brain shape asymmetries in human and chimpanzee brains. Biomedical Imaging: From Nano to Macro, 2011 IEEE International Symposium on, 2011b. IEEE, 310-316.
- GALABURDA, A. M., LEMAY, M., KEMPER, T. L. & GESCHWIND, N. 1978. Right-left asymmetries in the brain. *Science*, 199, 852-856.
- GANNON, P. J., HOLLOWAY, R. L., BROADFIELD, D. C. & BRAUN, A. R. 1998. Asymmetry of chimpanzee planum temporale: humanlike pattern of Wernicke's brain language area homolog. *Science*, 279, 220-222.
- GESCHWIND, N. & LEVITSKY, W. 1968. Human brain: left-right asymmetries in temporal speech region. *Science*, 161, 186-187.
- GOOD, C. D., JOHNSRUDE, I., ASHBURNER, J., HENSON, R. N., FRISTON, K. J. & FRACKOWIAK, R. S. 2001. Cerebral asymmetry and the effects of sex and handedness on brain structure: a voxel-based morphometric analysis of 465 normal adult human brains. *Neuroimage*, 14, 685-700.
- GRIMAUD-HERVÉ, D. 1997. *L'évolution de l'encéphale chez Homo erectus et Homo sapiens: exemples de l'Asie et de l'Europe*, CNRS ed. Paris.
- GUNZ, P. & MITTEROECKER, P. 2013. Semilandmarks: a method for quantifying curves and surfaces. *Hystrix, the Italian Journal of Mammalogy*, 24, 103-109.
- GUNZ, P., MITTEROECKER, P. & BOOKSTEIN, F. L. 2005. Semilandmarks in three dimensions. *Modern morphometrics in physical anthropology*. Springer.
- GUNZ, P., MITTEROECKER, P., NEUBAUER, S., WEBER, G. W. & BOOKSTEIN, F. L. 2009. Principles for the virtual reconstruction of hominin crania. *Journal of Human Evolution*, 57, 48-62.
- HARASTY, J., DOUBLE, K. L., HALLIDAY, G. M., KRIL, J. J. & MCRITCHIE, D. A. 1997. Language-associated cortical regions are proportionally larger in the female brain. *Archives of Neurology*, 54, 171.
- HERVÉ, P.-Y., CRIVELLO, F., PERCHEY, G., MAZOYER, B. & TZOURIO-MAZOYER, N. 2006. Handedness and cerebral anatomical asymmetries in young adult males. *Neuroimage*, 29, 1066-1079.
- HOLLOWAY, R. L. 1970. Australopithecine endocast (Taung specimen, 1924): A new volume determination. *Science*, 168, 966-968.

- HOLLOWAY, R. L. 1981. Volumetric and asymmetry determinations on recent hominid endocasts: Spy I and II, Djebel Irhoud I, and the Salé Homo erectus specimens, with some notes on neandertal brain size. *American Journal of Physical Anthropology*, 55, 385-393.
- HOLLOWAY, R. L. 1983a. Cerebral brain endocast pattern of *Australopithecus afarensis* hominid. *Nature*, 303, 420-422.
- HOLLOWAY, R. L. 1983b. Human paleontological evidence relevant to language behavior. *Human neurobiology*, 2, 105-114.
- HOLLOWAY, R. L. 1985. The past, present, and future significance of the lunate sulcus in early hominid evolution. *Hominid evolution: Past, present, and future*, 47-62.
- HOLLOWAY, R. L. 1986. Endocast morphology of Hadar hominid AL 162-28. *Nature*, 321, 536.
- HOLLOWAY, R. L. 1995. Toward a synthetic theory of human brain evolution. *Origins of the human brain*, 5, 42.
- HOLLOWAY, R. L. 2009. Brain fossils: endocasts. *Encyclopedia of neuroscience*, 2, 253-261.
- HOLLOWAY, R. L. 2015. Introduction: Paleoneurology, Resurgent! *Human Paleoneurology*. Springer.
- HOLLOWAY, R. L., BROADFIELD, D. C. & YUAN, M. S. 2003. Morphology and histology of chimpanzee primary visual striate cortex indicate that brain reorganization predated brain expansion in early hominid evolution. *The Anatomical Record Part A: Discoveries in Molecular, Cellular, and Evolutionary Biology*, 273, 594-602.
- HOLLOWAY, R. L., BROADFIELD, D. C., YUAN, M. S., SCHWARTZ, J. H. & TATTERSALL, I. 2004a. *The Human Fossil Record, Brain Endocasts--The Paleoneurological Evidence*, John Wiley & Sons.
- HOLLOWAY, R. L., CLARKE, R. J. & TOBIAS, P. V. 2004b. Posterior lunate sulcus in *Australopithecus africanus*: was Dart right? *Comptes Rendus Palevol*, 3, 287-293.
- HOLLOWAY, R. L. & DE LA COSTE-LAREYMONDIE, M. C. 1982. Brain endocast asymmetry in pongids and hominids: some preliminary findings on the paleontology of cerebral dominance. *American Journal of Physical Anthropology*, 58, 101-110.
- HOLLOWAY, R. L., SHERWOOD, C. C., HOF, P. R. & RILLING, J. K. 2009. Evolution of the brain in humans–Paleoneurology. *Encyclopedia of neuroscience*. Springer.
- JERISON, H. J. 1973. *Evolution of the Brain and Intelligence*, Academic Press.
- KELLER, S. S., HIGHLEY, J. R., GARCIA - FINANA, M., SLUMING, V., REZAIE, R. & ROBERTS, N. 2007. Sulcal variability, stereological measurement and asymmetry of Broca's area on MR images. *Journal of Anatomy*, 211, 534-555.
- KITCHELL, L. M. & SCHOENEMANN, P. T. Functional correlates of structural asymmetries in the human brain. *American Journal of Physical Anthropology*, 2014. WILEY-BLACKWELL 158.
- KITCHELL, L. M., SCHOENEMANN, P. T. & LOYET, M. Structural asymmetries in the human brain assessed via MRI. *American Journal of Physical Anthropology*, 2013. WILEY-BLACKWELL 167.

- KOCHETKOVA, V. I. 1978. *Paleoneurology*, VH Winston.
- KRIEGSTEIN, K. V. & GIRAUD, A.-L. 2004. Distinct functional substrates along the right superior temporal sulcus for the processing of voices. *Neuroimage*, 22, 948-955.
- LE GROS CLARK, W., COOPER, D. & ZUCKERMAN, S. 1936. The endocranial cast of the chimpanzee. *Journal of the Anthropological Institute of Great Britain and Ireland*, 249-268.
- LEMAY, M. 1976. Morphological cerebral asymmetries of modern man, fossil man, and nonhuman primate. *Annals of the New York Academy of Sciences*, 280, 349-366.
- LEMAY, M., BILLIG, M. S. & GESCHWIND, N. 1982. Asymmetries of the brains and skulls of nonhuman primates. *Primate brain evolution*. Springer.
- LEMAY, M. & KIDO, D. K. 1978. Asymmetries of the cerebral hemispheres on computed tomograms. *Journal of computer assisted tomography*, 2, 471-476.
- LUDERS, E., GASER, C., JANCKE, L. & SCHLAUG, G. 2004. A voxel-based approach to gray matter asymmetries. *Neuroimage*, 22, 656-664.
- MCHENRY, H. M. 1992. Body size and proportions in early hominids. *American Journal of Physical Anthropology*, 87, 407-431.
- MITTEROECKER, P. & GUNZ, P. 2009. Advances in geometric morphometrics. *Evolutionary Biology*, 36, 235-247.
- MOHR, J., PESSIN, M., FINKELSTEIN, S., FUNKENSTEIN, H., DUNCAN, G. & DAVIS, K. 1978. Broca aphasia Pathologic and clinical. *Neurology*, 28, 311-311.
- MONGE, J. & SCHOENEMANN, P. T. 2011. The Open Research Scan Archive (Orsa): A massive open-access archive of research quality computed tomography (CT) scans. *Pleistocene Databases: Acquisition, Storing, Sharing*, 4, 61-67.
- MONTGOMERY, S. H., CAPELLINI, I., BARTON, R. A. & MUNDY, N. I. 2010. Reconstructing the ups and downs of primate brain evolution: implications for adaptive hypotheses and *Homo floresiensis*. *BMC biology*, 8, 9.
- NAIR, D. G., PURCOTT, K. L., FUCHS, A., STEINBERG, F. & KELSO, J. S. 2003. Cortical and cerebellar activity of the human brain during imagined and executed unimanual and bimanual action sequences: a functional MRI study. *Cognitive brain research*, 15, 250-260.
- NEUBAUER, S. 2014. Endocasts: Possibilities and Limitations for the Interpretation of Human Brain Evolution. *Brain, behavior and evolution*, 84, 117-134.
- NEUBAUER, S., GUNZ, P. & HUBLIN, J.-J. 2010. Endocranial shape changes during growth in chimpanzees and humans: a morphometric analysis of unique and shared aspects. *Journal of human evolution*, 59, 555-566.
- NEUBAUER, S., GUNZ, P. & HUBLIN, J. J. 2009. The pattern of endocranial ontogenetic shape changes in humans. *Journal of Anatomy*, 215, 240-255.
- NITSCHKE, M. F., KLEINSCHMIDT, A., WESSEL, K. & FRAHM, J. 1996. Somatotopic motor representation in the human anterior cerebellum. *Brain*, 119, 1023-1029.
- PECHAUD, M., JENKINSON, M. & SMITH, S. 2006. BET2-MRI-Based Estimation of Brain, Skull and Scalp Surfaces. FMRIB Technical Report TR06MP1. Oxford, England: Oxford University.

- PHILLIPS, K. A. & HOPKINS, W. D. 2007. Exploring the relationship between cerebellar asymmetry and handedness in chimpanzees (*Pan troglodytes*) and capuchins (*Cebus apella*). *Neuropsychologia*, 45, 2333-2339.
- PILCHER, D. L., HAMMOCK, E. A. & HOPKINS, W. D. 2001. Cerebral volumetric asymmetries in non-human primates: A magnetic resonance imaging study. *Laterality: Asymmetries of Body, Brain and Cognition*, 6, 165-179.
- RADINSKY, L. B. 1979. *The fossil record of primate brain evolution*, American Museum of natural history.
- REDDY, D., KIM, J. & RAAUM, R. 2006. Resample.exe. NYCEP.
- SAMSON, S. & ZATORRE, R. J. 1994. Contribution of the right temporal lobe to musical timbre discrimination. *Neuropsychologia*, 32, 231-240.
- SCHOENEMANN, P. T. 1997. *An MRI study of the relationship between human neuroanatomy and behavioral ability*. University of California, Berkeley.
- SCHOENEMANN, P. T. 2006. Evolution of the size and functional areas of the human brain. *Annu. Rev. Anthropol.*, 35, 379-406.
- SCHOENEMANN, P. T. & BEGUN, D. 2013. Hominid brain evolution. *A Companion to Paleoanthropology*, 136-164.
- SCHOENEMANN, P. T., GEE, J., AVANTS, B., HOLLOWAY, R. L., MONGE, J. & LEWIS, J. 2007. Validation of plaster endocast morphology through 3D CT image analysis. *American journal of physical anthropology*, 132, 183-192.
- SHERWOOD, C. C., RILLING, J. K., HOLLOWAY, R. L. & HOF, P. R. 2009. Evolution of the Brain in Humans—Specializations in a Comparative Perspective. *Encyclopedia of neuroscience*. Springer.
- SLICE, D. E. 2007. Geometric morphometrics. *Annu. Rev. Anthropol.*, 36, 261-281.
- SMITH, G. E. 1913. The Piltdown Skull. *Nature*, 92, 131.
- STEINMETZ, H. & GALABURDA, A. M. 1991. Planum temporale asymmetry: In-vivo morphometry affords a new perspective for neuro-behavioral research. *Reading Disabilities*. Springer.
- STEPHAN, H., FRAHM, H. & BARON, G. 1981. New and revised data on volumes of brain structures in insectivores and primates. *Folia primatologica*, 35, 1-29.
- SUWA, G., KONO, R. T., SIMPSON, S. W., ASFAW, B., LOVEJOY, C. O. & WHITE, T. D. 2009. Paleobiological implications of the *Ardipithecus ramidus* dentition. *Science*, 326, 69-99.
- SYMINGTON, J. 1916. Endocranial casts and brain form: A criticism of some recent speculations. *Journal of anatomy and physiology*, 50, 111.
- THOMPSON, P. M., MEGA, M. S., VIDAL, C., RAPOPORT, J. L. & TOGA, A. W. Detecting Disease-Specific Patterns of Brain Structure Using Cortical Pattern Matching and a Population-Based Probabilistic Brain Atlas. *Information Processing in Medical Imaging*, 2001. Springer, 488-501.
- TOBIAS, P. V. 1975. Brain evolution in the Hominoidea. *Primate functional morphology and evolution*, 353-392.
- TOBIAS, P. V. 1987. The brain of *Homo habilis*: A new level of organization in cerebral evolution. *Journal of Human Evolution*, 16, 741-761.
- TOBIAS, P. V. 2001. Re - creating ancient hominid virtual endocasts by CT - scanning. *Clinical Anatomy*, 14, 134-141.
- TOGA, A. W. & THOMPSON, P. M. 2003. Mapping brain asymmetry. *Nature Reviews Neuroscience*, 4, 37-48.

- TUTTLE, R. H. 1986. *Apes of the world: Their social behavior, communication, mentality, and ecology*, Noyes Publications.
- VENN, O., TURNER, I., MATHIESON, I., DE GROOT, N., BONTROP, R. & MCVEAN, G. 2014. Strong male bias drives germline mutation in chimpanzees. *Science*, 344, 1272-1275.
- VENTRICE, F. 2011. *Modern Human Brain Growth and Development: Contribution to Brain Evolution in Hominids*.
- VON CRAMON-TAUBADEL, N., FRAZIER, B. C. & LAHR, M. M. 2007. The problem of assessing landmark error in geometric morphometrics: theory, methods, and modifications. *American Journal of Physical Anthropology*, 134, 24.
- WADA, J. A., CLARKE, R. & HAMM, A. 1975. Cerebral hemispheric asymmetry in humans: Cortical speech zones in 100 adult and 100 infant brains. *Archives of Neurology*, 32, 239-246.
- WATKINS, K. E., PAUS, T., LERCH, J. P., ZIJDENBOS, A., COLLINS, D. L., NEELIN, P., TAYLOR, J., WORSLEY, K. J. & EVANS, A. C. 2001. Structural asymmetries in the human brain: a voxel-based statistical analysis of 142 MRI scans. *Cereb Cortex*, 11, 868-77.
- WEBSTER, M. & SHEETS, H. D. 2010. A practical introduction to landmark-based geometric morphometrics. *Quantitative Methods in Paleobiology*, 16, 168-188.
- WERNICKE, C. 1874. *Der aphasische Symptomkomplex: eine psychologische Studie auf anatomischer Basis*, Cohn.
- ZELDITCH, M., SWIDERSKI, D., SHEETS, D. & FINK, W. 2004. Geometric Morphometrics for Biologists: A primer: Elsevier Academic Press. *Waltham, MA*.
- ZOLLIKOFER, C. P. E. & LEÓN, M. S. P. 2013. Pandora's growing box: inferring the evolution and development of hominin brains from endocasts. *Evolutionary Anthropology: Issues, News, and Reviews*, 22, 20-33.